Published for SISSA by Springer

Received: February 28, 2022
Revised: May 10, 2022
Accepted: May 23, 2022
Published: June 21, 2022

The muon $g-2$ anomaly confronts new physics in $e^{\pm}$ and $\mu^{\pm}$ final states scattering

Luc Darmé,[a,b] **Giovanni Grilli di Cortona**[b] **and Enrico Nardi**[b]

[a] *Institut de Physique des 2 Infinis de Lyon (IP2I), UMR5822, CNRS/IN2P3, F-69622 Villeurbanne Cedex, France*

[b] *Istituto Nazionale di Fisica Nucleare, Laboratori Nazionali di Frascati, C.P. 13, 00044 Frascati, Italy*

E-mail: l.darme@ip2i.in2p3.fr, grillidc@lnf.infn.it, Enrico.Nardi@lnf.infn.it

Abstract: The 4.2σ discrepancy between the standard model prediction for the muon anomalous magnetic moment a_μ and the experimental result is accompanied by other anomalies. A crucial input for the prediction is the hadronic vacuum polarization $a_\mu^{\rm HVP}$ inferred from $\sigma_{\rm had} = \sigma(e^+e^- \to \text{hadrons})$ data. However, the two most accurate determinations of $\sigma_{\rm had}$ from KLOE and BaBar disagree by almost $3\,\sigma$. Additionally, the combined data-driven result disagrees with the most precise lattice determination of $a_\mu^{\rm HVP}$ by $2.1\,\sigma$. We show that all these discrepancies could be accounted for by a new boson produced resonantly around the KLOE centre of mass energy and decaying promptly yielding e^+e^- and $\mu^+\mu^-$ pairs in the final states. This gives rise to three different effects: (i) the additional e^+e^- events will affect the KLOE luminosity determination based on measurements of the Bhabha cross section, and in turn the inferred value of $\sigma_{\rm had}$; (ii) the additional $\mu^+\mu^-$ events will affect the determination of $\sigma_{\rm had}$ via the (luminosity independent) measurement of the ratio of $\pi^+\pi^-\gamma$ versus $\mu^+\mu^-\gamma$ events; (iii) loops involving the new boson would contribute directly to the prediction for a_μ. We discuss in detail this possibility, and we present a simple model that can reconcile the KLOE and BaBar results for $\sigma_{\rm had}$, the data-driven and the lattice determinations of $a_\mu^{\rm HVP}$, the predicted and measured values of a_μ, while complying with all phenomenological constraints.

Keywords: New Light Particles, Specific BSM Phenomenology, New Gauge Interactions

ArXiv ePrint: 2112.09139

https://doi.org/10.1007/JHEP06(2022)122

JHEP06(2022)122

Contents

JHEP06(2022)122

1 Introduction

The recent experimental result for the muon anomalous magnetic moment a_μ from the FNAL Muon g-2 experiment [1] has confirmed the old BNL measurement [2], adding significance to the long standing discrepancy with the standard model (SM) prediction which is now raised to $4.2\,\sigma$. Currently, the world average for this discrepancy is

$$\Delta a_\mu \equiv a_\mu^{\rm exp} - a_\mu^{\rm SM} = (2.51 \pm 0.59) \cdot 10^{-9}\,, \tag{1.1}$$

where $a_\mu^{\rm exp}$ is the combined result from refs. [1, 2], and the SM estimate is the one recommended by the *Muon g-2 Theory Initiative* [3] which is mainly based on the estimates in refs. [4–23]. This estimate relies on a data-driven approach that makes use of experimental measurements of the $\sigma_{\rm had} \equiv \sigma(e^+e^- \to \text{hadrons})$ cross section to determine the hadronic

vacuum polarization contribution $a_\mu^{\rm HVP}$. This is the most uncertain input in the prediction for a_μ and, due to its non-perturbative nature, improving in precision is a difficult task. Apart for the uncertainty, one can also wonder to which level the adopted value can be considered reliable, since determinations of $a_\mu^{\rm HVP}$ using data from different experiments exhibit a certain disagreement. In particular, KLOE [24] and BaBar [25] disagree at the level of $3\,\sigma$, especially in the $\pi^+\pi^-$ channel that accounts for more than 70% of the value of $a_\mu^{\rm HVP}$, and while BaBar data favour smaller values of Δa_μ, KLOE data pull to increase the discrepancy.[1]

The HVP contribution can also be determined from first principles by means of lattice QCD techniques. However, until recently, the uncertainties in lattice results were too large to allow for useful comparisons with the data-driven determination. A first lattice QCD computation of $a_\mu^{\rm HVP}$ with subpercent precision was recently accomplished by the BMW collaboration [31] $a_\mu^{\rm HVP} = 707.5(5.5) \times 10^{-10}$. The result differs from the world average obtained from the data-driven dispersive approach by $2.1\,\sigma$ [32] and, in particular, it would yield a theoretical prediction for a_μ only $1.3\,\sigma$ below the measurement.[2]

We can thus conclude that the muon $g-2$ anomaly eq. (1.1) is accompanied by other discrepancies that, although of lesser significance, can shed some suspicion on interpreting the a_μ anomaly as a reliable hint of new physics (NP). In this respect, new high statistics measurements of $\sigma_{\rm had}$, and in particular in the $\pi^+\pi^-$ channel, that might be soon provided by the CMD-3 collaboration [34], as well as new high precision lattice evaluations, which might confirm or correct the BMW result [31], will be of crucial importance not only to strengthen or resize the evidences for a $(g-2)_\mu$ anomaly, but also to assess the status of the related additional discrepancies. In the meantime, it is worthwhile wondering if the discordant determinations of $a_\mu^{\rm HVP}$ (KLOE vs. BaBar and $\sigma_{\rm had}$ vs. lattice) could be explained, jointly with Δa_μ, within a single NP scenario. In this paper we explore this possibility.

We suggest that the origin of the KLOE-BaBar discrepancy could be due to a NP contribution from a hypothetical new resonance V lying close to the ϕ mass. This resonance decays semi-visibly into charged leptons plus additional dark sector particles, collectively denoted as X, thus producing a certain number of e^+e^- and $\mu^+\mu^-$ events with a smooth continuous spectrum. Electron-positron pairs would contribute to Bhabha scattering events, which are used by the experimental collaborations to determine the beam luminosity by comparing the measured number of e^+e^- events with the QED prediction. Clearly, in those cases in which $\sigma_{\rm had}$ is determined directly from the number of hadronic events [35], not accounting for such a NP contribution to Bhabha scattering would result in overestimating the luminosity and hence underestimating $\sigma_{\rm had}$.

On the other hand, events from $e^+e^- \to V \to \mu^+\mu^- X$ would be interpreted as $e^+e^- \to \gamma^*\gamma_{\rm ISR} \to \mu^+\mu^-\gamma_{\rm ISR}$ events in the analyses in which the Initial State Radiation (ISR) photon goes undetected [36, 37], and would be counted as originating from processes involving γ^* virtual photon exchange, resulting in an overestimation of the $\sigma_{\mu\mu\gamma}$ cross section from pure QED. Similarly, events from $e^+e^- \to \gamma V \to \gamma\mu^+\mu^- X$ can also mimic

[1] Due to relatively larger errors, there is instead agreement within $1.5\,\sigma$ between KLOE and CMD-2 [26–28], SND [29], BES-III [30].

[2] Other lattice determinations also tend to give larger $a_\mu^{\rm HVP}$ central values although with considerably larger errors, see e.g the review [33].

JHEP06(2022)122

pure QED ISR events in which the photon is detected [30, 37], when the missing energy cannot be precisely reconstructed due to experimental limitations. This would affect the determination of $\sigma_{\rm had}$ based on the ratio between the number of $\pi^+\pi^-(\gamma)$ and $\mu^+\mu^-(\gamma)$ events [36], since $\sigma_{\rm had} \propto \sigma_{\pi\pi\gamma}/\sigma^{\gamma^*}_{\mu\mu\gamma} > N_{\pi\pi\gamma}/N_{\mu\mu\gamma}$, where $\sigma^{\gamma^*}_{\mu\mu\gamma}$ denotes the pure QED process that should be used to determine the photon HVP contribution (see eq. (2.8) below). If these (hypothetical) NP effects are instead included, the KLOE vs. BaBar discrepancy can be solved, and the disagreement between the data-driven and the lattice determination of $a_\mu^{\rm HVP}$ can also be explained.

As a concrete example, we discuss a simple model originally proposed as a realisation of the "inelastic dark matter" mechanism [38–41], in which the contribution to the Bhabha process $e^+e^- \to e^+e^-$ of a new vector boson V of mass $m_V \sim 1\,\text{GeV}$ can result in an overestimation of the luminosity at KLOE, with negligible effects on the luminosity determination in other experiments. Furthermore, the contribution of NP-related muonic events $e^+e^- \to (\gamma_{\rm ISR})V \to (\gamma_{\rm ISR})\mu^+\mu^- X$ will affect the analyses that rely on the ratio $N_{\pi\pi\gamma}/N_{\mu\mu\gamma}$ to determine $\sigma_{\rm had}$. In this model, the values of the parameters required to account for the KLOE vs. BaBar discrepancy and for reconciling the data-driven vs. lattice determination of $a_\mu^{\rm HVP}$ do not conflict with other experimental constraints (mono-photon search in BaBar, ϕ-related observables, etc. . .). The strongest constraints come from the KLOE measurement of $\sigma_{\rm had}$ carried out at a center of mass (CoM) energy slightly below the ϕ resonance (KLOE10) [42], and from the measurement of the forward-backward asymmetry in e^+e^- final states [43]. Yet, these constraints are not sufficiently strong to exclude neither our model, nor the general NP mechanism underlying it. While the indirect effects of the new V boson outlined above are still unable to fully account for the Δa_μ discrepancy, due to the coupling between V and the muons there is also a direct contribution to a_μ from loops involving V. This direct effect suffices to bring the theoretical estimate of the muon anomalous magnetic moment in agreement with the experimental measurement. Thus, a single NP input is able to solve consistently all the a_μ-related anomalies at once.

The paper is structured as follows. In section 2 we first review the main ingredients of the data-driven calculation of $a_\mu^{\rm HVP}$, then we illustrate the mechanism through which a shift in the luminosity determination can affect the KLOE result for $\sigma_{\rm had}$, and finally we discuss the modification of $\sigma_{\rm had}$ from NP contributions to $e^+e^- \to \mu^+\mu^-\gamma$. In section 3 we put forth an explicit realisation based on an inelastic dark matter model, we study quantitatively the different effects and we present all the details of the numerical analysis. section 4 is devoted to an analysis of the existing phenomenological constraints on our NP model. In section 5 we discuss the solution to the a_μ-related anomalies, and finally in section 6 we resume the main results and we draw the conclusions.

2 The muon magnetic moment and the hadronic cross-section

2.1 Data-driven calculation of $a_\mu^{\rm HVP}$

At leading order, the contribution to the muon magnetic moment arising from the hadronic vacuum polarisation can be derived from the data on the hadronic cross-section

JHEP06(2022)122

$\sigma_{\rm had} = \sigma(e^+e^- \to \text{hadrons}\,(\gamma))$ by means of the optical theorem [44, 45]

$$a_\mu^{\rm LO,HVP} = \frac{1}{4\pi^3}\int_{4m_\pi^2}^{\infty} ds\, K(s)\sigma_{\rm had}(s)\,. \tag{2.1}$$

Here, $\sigma_{\rm had}$ is the bare $e^+e^- \to \gamma^* \to \text{hadrons}\,(\gamma)$ cross-section, obtained by removing the infinite string of hadronic vacuum polarisation insertions in the photon propagator (that leads to the running of $\alpha_{\rm QED}$), and the kernel function reads

$$K(x) = \frac{x^2}{2}(2-x^2) + \frac{1+x}{1-x}x^2\log x + \frac{(1+x^2)(1+x)^2}{x^2}\left(\log(1+x) - x + \frac{x^2}{2}\right)\,, \tag{2.2}$$

with $x = (1-\beta_\mu)/(1+\beta_\mu)$ and $\beta_\mu = \sqrt{1-4m_\mu^2/s}$. On the basis of the analyses in refs. [8–13], the *Muon g-2 Theory Initiative* [3] has recommended the numerical value

$$a_\mu^{\rm LO,HVP} = 693.1 \pm 4.0 \cdot 10^{-10}\,, \tag{2.3}$$

which directly depends on the accuracy of the hadronic cross-section experimental determination. Indeed, the HVP contribution to the muon anomalous magnetic moment is a widely studied subject (recent works include refs. [10, 12, 13, 46–48]). In general, various data-sets coming from the same or different experiments and exploiting several final states must be combined. The most important channel is the $\pi^+\pi^-$ channel which accounts for more than 70% of $a_\mu^{\rm LO,HVP}$. Many experimental measurements have been performed, leading to the embarrassing situation in which the two most precise measurements disagree at the level of $\sim 3\sigma$. Indeed, the values of $a_\mu^{\rm LO,HVP}$ reported by KLOE as the average of their three different analyses [24] and BABAR [25, 37] show a worrisome difference, while other experiments (CMD-2, BESIII, SND [26–30]) have reported results that lie in between these two, albeit with larger uncertainties. Note that any effect that could lift the overall value of $\sigma_{\rm had}$ given by KLOE, besides reducing the discrepancy with BaBar, at the same time would also reduce Δa_μ.[3]

2.2 Modifying the hadronic cross-section: the luminosity determination

Some of the early experimental results for the hadronic cross-section (and in particular the two first analysis from the KLOE collaboration [35, 42], denoted respectively as KLOE08 and KLOE10) depend on the specific luminosity $\mathcal{L}_{e^+e^-}$ of the colliding beams: $\sigma_{\rm had} \propto N_{\rm had}/\mathcal{L}_{e^+e^-}$, with $N_{\rm had}$ the number of hadronic events. The luminosity is estimated by comparing high statistics measurements of $e^+e^- \to e^+e^-$ events with the SM prediction for Bhabha scattering:

$$\mathcal{L}_{e^+e^-}^{\rm SM} = \frac{N_{\rm Bha}}{\sigma_{\rm eff}^{\rm SM}}, \tag{2.4}$$

where $N_{\rm Bha}$ is the total number of (background subtracted) Bhabha events. For each experiment, the effective SM Bhabha cross section $\sigma_{\rm eff}^{\rm SM}$ is evaluated by inserting into

[3] $a_\mu^{\rm HVP}$ can be also estimated from hadronic τ decays data [46, 49–52]. The resulting value $(703.0 \pm 4.4) \times 10^{-10}$ [51] is significantly larger than the result from $e^+e^- \to$ hadrons, and in agreement with the lattice estimate.

JHEP06(2022)122

detector simulations the results of high precision Bhabha event generators [53–55]. The presence of NP contributions to $e^+e^- \to e^+e^-$ unaccounted for by $\sigma_{\rm eff}^{\rm SM}$ would then yield an incorrect estimate of the beam luminosity. The true luminosity $\mathcal{L}_{e^+e^-}$ would be related to the inferred one as

$$\mathcal{L}_{e^+e^-} = \mathcal{L}_{e^+e^-}^{\rm SM} \frac{\sigma_{\rm eff}^{\rm SM}}{\sigma_{\rm eff}}\,, \tag{2.5}$$

where $\sigma_{\rm eff}$ is the full Bhabha cross-section including the NP contribution, that we parametrize in terms of a correction to the QED Bhabha cross section as

$$\sigma_{\rm eff} = \sigma_{\rm eff}^{\rm SM}(1+\delta_R)\,. \tag{2.6}$$

Note that a possible difference in the efficiencies for revealing SM and NP-related events is also absorbed in δ_R. As a consequence, the true luminosity would be smaller (cf. eq. (2.5)), the true hadronic cross section would become larger $\sigma_{\rm had} \to \sigma_{\rm had}(1+\delta_R)$, and thus the inferred value of the HVP would be increased as:

$$a_\mu^{\rm LO,HVP} \to a_\mu^{\rm LO,HVP}\,(1+\delta_R)\,. \tag{2.7}$$

It is understood that the correction δ_R induced by the shift in the luminosity depends on the details of the experimental setup, in such a way that while it can be quite important in some experiment, it could be completely negligible in others. Needless to say, lattice calculations of $a_\mu^{\rm HVP}$ are not affected by this type of indirect effects on $a_\mu^{\rm LO,HVP}$ that stem from modifications of the estimated luminosity.

2.3 Modifying the hadronic cross-section: the $\sigma(\mu\mu\gamma)$ method

Several experimental measurements, including KLOE12 [36], BaBar [37] and BESIII [30] do not rely on a determination of the luminosity from Bhabha scattering to measure $\sigma_{\rm had}$, and use instead a luminosity independent method. The method exploits the following relation

$$\sigma^0_{\pi^+\pi^-} = \frac{N_{\pi^+\pi^-\gamma_{\rm ISR}}}{N_{\mu^+\mu^-\gamma_{\rm ISR}}}\,\sigma^0_{\mu^+\mu^-}\,, \tag{2.8}$$

that involves the ratio between the number of $\pi^+\pi^-$ and $\mu^+\mu^-$ events with an ISR photon, and the $\sigma^0_{\mu^+\mu^-} \equiv \sigma(e^+e^- \to \mu^+\mu^-)$ cross section computed in QED. The KLOE12 measurement is peculiar in that it does not detect the photon, since the angular cuts that are used to enhance ISR over final state radiation (FSR) events imply that the photon gets lost in the beam pipe. The CoM energy of the collision is then reconstructed from the charged particles invariant mass.

If we have an excess of NP-related $\mu\mu X$ events (where X represents undetected particles) mimicking $\mu\mu\gamma$ final states and contributing to the denominator in eq. (2.8), these events need to be subtracted out in order that the derived value of $\sigma^0_{\pi^+\pi^-}$ could be correctly related to the photon HVP. The hadronic cross-section induced by virtual photon exchange is then shifted as

$$\sigma^0_{\pi^+\pi^-} \quad \longrightarrow \quad \sigma^{0\,(\gamma^*)}_{\pi^+\pi^-} \simeq \sigma^0_{\pi^+\pi^-}\left[1+\delta_\mu(s')\right]\,, \tag{2.9}$$

JHEP06(2022)122

where s' is the invariant mass squared of the charged particles, and we have defined:

$$\delta_\mu(s') \equiv \frac{\sigma^{\rm NP}_{\mu\mu X}(s')}{\sigma_{\mu\mu}(s')} \frac{\epsilon^{\rm NP}}{\epsilon^{\rm SM}} \,, \tag{2.10}$$

where $\epsilon^{\rm NP}$ ($\epsilon^{\rm SM}$) is the efficiency of the selection cuts for the NP (SM) events. The cross section $\sigma^{\rm NP}_{\mu\mu X}$ represents the NP contribution yielding events for which the final state may contain additional (invisible) states, and that are counted in the experimental analysis as long as they pass the kinematic cuts.

The shift in the hadronic cross section depends on s' and has to be integrated along with the kernel function $K(s')$ in order to obtain the final shift to $a_\mu^{\rm LO,HVP}$. A similar correction will also affect every measurement which uses the di-muon final state as a luminosity measurement. Finally, a flavour-universal new physics effect capable of modifying the large angle $e^+e^- \to e^+e^-$ cross-section at the level of a few percent, can in principle lead to an effect of similar size for $\gamma\mu\mu X$ events, where an ISR photon is emitted, up to differences related to the muon mass and to different experimental cuts. Therefore we can expect the correction δ_R of the previous section and the correction δ_μ discussed in this section to be of a similar size.

A remark is in order regarding the possibility that the NP will also produce an excess of hadronic events. Since these events will not be related to the exchange of a virtual γ^*, they must be subtracted from the hadronic data sample in order to reconstruct the $\sigma^{0\,(\gamma^*)}_{\pi^+\pi^-}$ cross section from which the photon HVP can then be derived. Let us define in complete analogy with eq. (2.10) a correction

$$\delta_\pi(s') \equiv \frac{\sigma^{\rm NP}_{\pi\pi X}(s')}{\sigma_{\pi\pi}(s')} \frac{\epsilon^{\rm NP}}{\epsilon^{\rm SM}} \,. \tag{2.11}$$

The effect of the $\pi\pi$ events of NP origin can then be subtracted out simply by replacing in eq. (2.6) (and in eq. (2.7)) $\delta_R \to \delta_R - \delta_\pi(s')$, and in eq. (2.9) $\delta_\mu(s') \to \delta_\mu(s') - \delta_\pi(s')$. It is clear that the relative strength characterising the NP couplings to the leptons and to the hadrons is a model dependent issue, so that the size of the hadronic shift δ_π relative to the leptonic ones δ_R, δ_μ cannot be assessed in a general way. However, in our signal region, corresponding to the ρ/ω resonance, the SM cross-section for hadronic final states is larger than the one for muons by about an order of magnitude. Therefore, in models where the NP contribution to the leptonic and hadronic channels are of similar size, we have $\delta_R \sim \delta_\mu(s') \gg \delta_\pi(s')$. This will be the case in the example that will be detailed below, where in first approximation the hadronic shift can be neglected, and we can simply set $\delta_\pi(s') \approx 0$.

2.4 Overall effects of new physics on $a_\mu^{\rm HVP}$

Several experiments have provided measurements of the hadronic cross section. Combining these measurements is an intricate process which requires the use of dedicated codes, which are not publicly available [12, 13]. In order to get a handle of the soundness of the numerical procedure that we have adopted, we have relied on the available results for the various experiments reported in refs. [12, 13], focusing on the range $\sqrt{s'} \in [0.6, 0.9]$ GeV for the

JHEP06(2022)122

reduced energy:

$$a_\mu^{\rm HVP}(\sqrt{s'} \in [0.6, 0.9]\,{\rm GeV}) = \begin{cases} (366.9 \pm 2.1) \cdot 10^{-10} & ({\rm KLOE}) \\ (376.8 \pm 2.7) \cdot 10^{-10} & ({\rm BABAR}) \\ (372.5 \pm 3) \cdot 10^{-10} & ({\rm CMD\text{-}2}) \\ (368.3 \pm 4.2) \cdot 10^{-10} & ({\rm BESIII}) \\ (371.8 \pm 5) \cdot 10^{-10} & ({\rm SND}) \\ (377.0 \pm 6.3) \cdot 10^{-10} & ({\rm CLEO})\,. \end{cases} \tag{2.12}$$

When combined with a simple χ^2, we obtain a global fit of $a_\mu^{\rm HVP}(\sqrt{s'} \in [0.6, 0.9]\,{\rm GeV}) = 371.1$ that matches the results of both the combined fit presented in refs. [12, 13] (see also table 6 in ref. [3]), thus corroborating the reliability of our method.

Feeding the indirect effects of NP discussed in sections 2.2 and 2.3 into the results listed in eq. (2.12) is far from being a straightforward step. This is because different measurements are affected by the NP in different ways, while others are not affected at all. In particular, the KLOE result in eq. (2.12) corresponds to an average of three different analyses, labelled as KLOE08 [35], KLOE10 [42] and KLOE12 [36]. A NP-related shift in the luminosity determination (see section 2.2) can affect KLOE08 and KLOE10, but not KLOE12. This last analysis can instead be affected by additional NP-related $\mu^+\mu^-$ events (see section 2.3). The rest of this section is thus devoted to unfold the details of the indirect NP effects on the three KLOE analyses.

The hadronic cross section $\sigma^0_{\pi\pi}(s')$, whose determination was the aim of the KLOE analyses, is related to the radiative cross section that includes the emission of an ISR photon via the following relation:

$$s\frac{d\sigma(\pi^+\pi^-\gamma)}{ds'} = \sigma^0_{\pi\pi}(s')H(s', s), \tag{2.13}$$

where H is the radiator function that accounts for the ISR and $s' = M^2_{\pi\pi}$ is the di-pion invariant mass. The different strategies followed by the KLOE collaboration in their three different analysis are resumed as follows:

- KLOE08 data-set consists on 60 measurements in the range $0.35 < s'/{\rm GeV}^2 < 0.85$ collected with the e^+e^- beam energies tuned to $\sqrt{s} = 1.0194\,{\rm GeV}$, that is at the ϕ-meson pole. Their determination of $\sigma^0_{\pi\pi}$ relies directly on eq. (2.13), where the radiative cross section in the LH side is inferred from the number of $\pi^+\pi^-\gamma$ events that pass the cuts, and relies on the knowledge of the luminosity that, as discussed in section 2.2, is measured via Bhabha scattering.

- KLOE10 data-set consists of 75 measurements of the radiative cross section in the range $0.1 < s'/{\rm GeV}^2 < 0.85$, collected with the e^+e^- beam energies tuned to $\sqrt{s} = 1\,{\rm GeV}$, that is about $4.5 \times \Gamma_\phi$ below the ϕ pole. Also in this case the inferred hadronic cross section depends on the measurement of the luminosity. However, given the $\sim 20\,{\rm MeV}$ difference in the CoM energy with respect to KLOE08, the two measurements could

JHEP06(2022)122

be simultaneously affected by a luminosity redetermination only if the width of the new resonance is several times larger than Γ_ϕ. The model discussed in the next section yields instead a width of order Γ_ϕ. Then it turns out that the most convenient choice is that of shifting KLOE08 results by locating the new resonance close to m_ϕ, while leaving the KLOE10 measurement unaffected by the NP.

- KLOE12 relies instead on eq. (2.8) where data correspond to the ratio between the number of $\pi^+\pi^-\gamma$ and $\mu^+\mu^-\gamma$ events (where the photon goes undetected) measured in 30 different bins in the interval $0.35 < s'/\text{GeV}^2 < 0.95$, where s' corresponds to the $\mu\mu$ and $\pi\pi$ invariant mass. The advantage of this method is that the dependence on the luminosity cancels in the ratio, so that KLOE12 is not affected by possible changes in the luminosity determination. However, as described in section 2.3, the measurement would be directly affected by additional $\mu^+\mu^-$ events of NP origin accompanied by undetected X particle(s).

In the invariant mass squared range in which the three KLOE analyses overlap, the numerical results for the individual contribution to the muon magnetic anomaly are [24]:

$$a_\mu^{\text{HVP}}(s' \in [0.35, 0.85]\,\text{GeV}^2) = \begin{cases} (378.9 \pm 3.2) \cdot 10^{-10} & (\text{KLOE08}) \\ (376.0 \pm 3.4) \cdot 10^{-10} & (\text{KLOE10}) \\ (377.4 \pm 2.6) \cdot 10^{-10} & (\text{KLOE12})\,, \end{cases} \tag{2.14}$$

We use these determinations and, after correcting them for the effects of δ_R (luminosity shift) and δ_μ ($\mu\mu$ events of NP origin) we combine them into a single KLOE result.[4]

While we have so far not specified an explicit NP mechanism responsible for the indirect corrections, we anticipate that we have in mind the excitation of a new resonance which promptly decays, yielding the required excess of e^+e^- and $\mu^+\mu^-$ pairs possibly accompanied by other undetected particles. As a consequence, a measurement performed at a CoM energy below the NP resonance would remain unaffected by these corrections. However, experiments that exploit the ISR method to scan over the reduced energy $\sqrt{s'}$ will generally be affected whenever the CoM energy $\sqrt{s}$ is above the resonance, even if not particularly close to the pole. This is because ISR photon emission can downgrade the effective e^+e^- collision energy to the right value to excite the resonance. Hence, for example, the BESIII measurement ($\sqrt{s} \simeq 3.8\,\text{GeV}$, $\sqrt{s'} \in [0.6,\, 0.9]\,\text{GeV}$) would be affected by a new resonance sitting close to the ϕ mass, and in our study we have taken this effect into account. BaBar data-taking was carried out at $\sqrt{s} \simeq 10.6\,\text{GeV}$, and $a_\mu^{\text{LO,HVP}}$ was calculated using the measured $\pi^+\pi^-$ cross section from threshold to 1.8 GeV, and in this case the high energy bins would clearly not get affected by a resonance at the ϕ mass. Conservatively, we have not included in our main results a possible correction to the BaBar measurements, even for

[4] As discussed in [24] there are large correlations among the three different KLOE determinations of a_μ^{HVP}. Most sources of systematic uncertainties, which represent the leading contribution to the total error, are fully correlated between all energy bins. There is also a full statistical correlation in the two-pion data that are shared between KLOE08 and KLOE12 [24]. We defer to future work the complete analysis of the KLOE datasets corresponding to a total of 195 data bins along with their correlation matrices.

JHEP06(2022)122

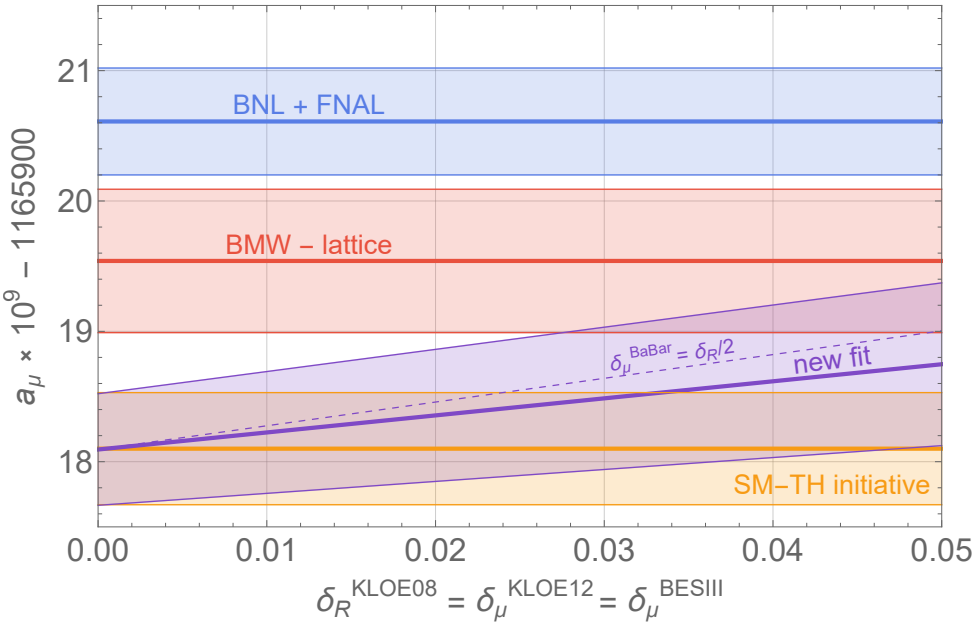

Figure 1. Theoretical prediction for a_μ based on a data driven global fit to $a_\mu^{\rm LO,HVP}$ obtained by including a NP correction affecting in an equal way e^+e^- and $\mu^+\mu^-\gamma$ final states (oblique violet band). The thick purple line assumes that the NP does not affect the BaBar result, while the dotted purple line assumes for BaBar an effect half the size than the one in KLOE and BESIII. The blue band corresponds to the combined BNL and FNAL experimental results, the red band to the prediction obtained with the BMW lattice estimate of $a_\mu^{\rm LO,HVP}$ [31], and the orange band to the one obtained from $\sigma_{\rm had}$ in the absence of NP corrections. The width of the bands represent $1\,\sigma$ uncertainties.

the subset of data restricted to the $\sqrt{s'}$ interval in eq. (2.12). However, to get an handle on the possible consequence of shifting also the BaBar measurement, we will show the effects of assuming a correction half the size the one for BESIII.

Finally, we should also stress that our analysis has been forcefully restricted to the invariant mass squared interval $0.35 \leq s'/{\rm GeV}^2 \leq 0.85$ for which we could carry out our procedure in a consistent way. However, since the contribution of the $e^+e^- \to \pi^+\pi^-$ channel to $a_\mu^{\rm HVP}$ over the complete $\sqrt{s'}$ range is about 35% larger, we expect that a full fit using the dedicated (but non-public) codes from [12, 13] could lead to a sizeably larger shift in $a_\mu^{\rm LO,HVP}$. This means that the results we are presenting here can be taken as a conservative estimate of the possible NP effects on the $a_\mu^{\rm HVP}$ determination.

We illustrate the results of our fit in figure 1. The blue band corresponds to the combined BNL and FNAL experimental results, the red band to the prediction obtained with the BMW lattice estimate of $a_\mu^{\rm LO,HVP}$ [31], and the orange band to the one obtained from $\sigma_{\rm had}$ without modifications of the KLOE and BESIII results. The excellent agreement between our χ^2 fit and the full results of refs. [12, 13] is put in evidence by the precise overlap between the violet and the orange bands occurring at the left boundary of figure 1, where the KLOE and BESIII results are taken at face value and not modified. We next increase the KLOE08, KLOE12 and BESIII value for $\sigma_{\rm had}$ assuming this is due to some

JHEP06(2022)122

unspecified NP contribution that affects the luminosity measurement (KLOE08) and the detected number of $\mu\mu\gamma$ events (KLOE12 and BESIII), while it remains negligible for all the other measurements. The purple band shows how a 2–3% shift of equal size in KLOE08, KLOE12 and BESIII would yield a shift of $\sim 0.5 \times 10^{-9}$ in $a_\mu^{\rm LO,HVP}$, and would drive the dispersive determination of $a_\mu^{\rm LO,HVP}$ in agreement at the $\sim 1.5\sigma$ level with the BMW-lattice result. As will be discussed in the following sections, a moderate shift of this size would also maintain the different KLOE analyses in overall satisfactory agreement among them.

On the other hand, in order to reduce to the $\sim 1\,\sigma$ level the tension with the combined BNL and FNAL experimental results, $a_\mu^{\rm LO,HVP}$ must be increased by an appreciably larger factor $\sim 1.6 \cdot 10^{-9}$. However, this would bring the KLOE08 and KLOE12 results in serious disagreement with KLOE10, and KLOE12 data on $\mu\mu\gamma$ will also get in strong tension with the SM prediction. Finally, the dotted purple line assumes a shift for BaBar of half the size the one in BESIII and KLOE.

To summarise, a NP effect acting only indirectly through a luminosity shift (KLOE08) and via the production of an excess of $\mu\mu\gamma$ events (KLOE12 and BESIII) would suffice to reinstate a satisfactory agreement between the different experimental determinations of $\sigma_{\rm had}$, and to reconcile the dispersive data-driven and lattice estimates of $a_\mu^{\rm LO,HVP}$. Yet, it would not be able to fully solve the discrepancy between the measured value of a_μ and the theoretical prediction, which thus still calls for a direct NP contribution to the muon anomalous magnetic moment. In the next section we will present and explicit example in which a new Feebly Interacting Particle (FIPs) produced resonantly at the KLOE08/KLOE12 CoM energy and decaying mostly "semi-visibly" into e^+e^- and $\mu^+\mu^-$, can produce indirect effects of the required size, while a direct loop contribution of the FIP to the muon anomalous magnetic moment can eventually solve all the a_μ-related anomalies.

3 Model realisation and analysis

In section 3.1 we describe a simple model, that fits in the so-called "inelastic dark matter (iDM) scenario", which is well suited to increase the number of Bhabha events in KLOE08 and to provide additional $\mu^+\mu^-$ events in KLOE12, while evading at the same time all other experimental constraints. In section 3.2 we first review the details of the luminosity measurements in the different experiments that contributed to the determination of $\sigma_{\rm had}$, and then we analyse quantitatively the effects on the determination of $a_\mu^{\rm LO,HVP}$ from $\sigma_{\rm had}$ data that could result from an overestimation of the KLOE luminosity. In section 3.3 we study the effects of additional NP-related $\mu\mu X$ events at KLOE12.

3.1 An inelastic dark matter model

We introduce a "dark" Abelian gauge group $\mathrm{U}(1)_D$ with gauge coupling g_D, along with a dark Higgs S with $\mathrm{U}(1)_D$-charge $q_S = +2$, and two Weyl spinors η, ξ with charges $q_\eta = -q_\xi = -1$ that can be combined in a Dirac fermion $\chi = (\eta\ \xi^\dagger)^T$. We furthermore assume that a charge conjugation symmetry extended to the dark sector enforces invariance under the transformations $V \to -V$, $\eta \to \xi^\dagger$ and $\xi^\dagger \to \eta$ [41].

JHEP06(2022)122

Under these premises, we can write the following Lagrangian terms:

$$\mathcal{L}_V = -\frac{1}{4}F'^{\mu\nu}F'_{\mu\nu} - \frac{g'\varepsilon}{\cos\theta_w}V_\mu \mathcal{J}^\mu_Y\,, \tag{3.1}$$

$$\mathcal{L}_S = (D^\mu S)^\dagger (D_\mu S) + \mu_S^2|S|^2 - \frac{\lambda_S}{2}|S|^4 - \frac{\lambda_{SH}}{2}|S|^2|H|^2\,, \tag{3.2}$$

where we have introduced the customary kinetic mixing term ε corresponding to a small interaction between the dark photon V_μ and the hypercharge current $\mathcal{J}^\mu_Y$ [56, 57]. The Lagrangian for the dark fermions can be written as

$$\mathcal{L}^{\rm DM} = \bar{\chi}\left(i\not{\partial} - m_\chi\right)\chi - \frac{1}{2}y_S S(\eta^2 + {\xi^\dagger}^2) + \text{ h.c.} \tag{3.3}$$

where the second term describes the coupling between the Weyl fermions and the dark Higgs boson S. Note that the charge conjugation symmetry mentioned above enforces that both η and $\xi^\dagger$ couple to S with the same Yukawa coupling. The dark Higgs boson mass m_S and the dark photon mass m_V read

$$m_S = \sqrt{2\lambda_S}\,v_S\,, \tag{3.4}$$

$$m_V = 2g_D v_S = \left(\frac{\sqrt{2}g_D}{\sqrt{\lambda_S}}\right) m_S\,. \tag{3.5}$$

The diagonalisation of the fermion mass matrix is straightforward and leads to two states $\chi_1 = \frac{i}{\sqrt{2}}(\eta - \xi)$ and $\chi_2 = \frac{1}{\sqrt{2}}(\eta + \xi)$ with masses

$$m_{\chi_1,\chi_2} = m_\chi \mp \frac{1}{\sqrt{2}}y_S v_S\,. \tag{3.6}$$

The phase of χ_1 has been fixed to obtain a positive mass term under the assumption $m_\chi \gtrsim y_S v_S/\sqrt{2}$. In the mass basis, the dark Higgs S couples diagonally to $\chi_{1,2}$ (expressed in term of the Majorana spinors) via the term:

$$\mathcal{L}_{S\chi} = -\frac{1}{2}y_S\, S\,(\chi_2^2 - \chi_1^2)\,, \tag{3.7}$$

where the Yukawa coupling can be expressed as

$$y_S = \frac{g_D}{\sqrt{2}}\frac{m_{\chi_2} - m_{\chi_1}}{m_V} \tag{3.8}$$

In contrast, the dark photon interacts with the fermions via an off-diagonal coupling

$$\mathcal{L}_{V\chi} = -ig_D V_\mu \bar{\chi}_2 \gamma^\mu \chi_1\,. \tag{3.9}$$

This construction can satisfy the main conditions to generate a significant shift in the KLOE luminosity estimate and to provide additional di-muon events, while escaping detection in other experiments:

- the dark photon mass must be very close to the KLOE CoM energy $\sqrt{s} \simeq 1.02\,\text{GeV}$, in order to produce V resonantly;

JHEP06(2022)122

- dark photon decays must contribute non-negligibly to Bhabha scattering events, and therefore they need to include e^+e^- pairs with invariant mass close to 1 GeV, as well as additional di-muon events;

- in order to escape bump searches, the dark photon main decay channel must be multi-body and must include some missing energy.

We can choose $m_V \sim 1\,\text{GeV} \gtrsim m_{\chi_2} \gg m_{\chi_1}$ by fixing v_S and by requiring the approximate relations

$$y_S v_S \sim \sqrt{2} m_\chi \,, \quad \sqrt{2} y_S \lesssim g_D \,. \tag{3.10}$$

When this arrangement of mass values is satisfied, the dark photon decays mainly proceed through the chain $V \to \chi_1\,\chi_2 \to \chi_1\,\chi_1\,e^+e^-$ ($\mu^+\mu^-$). That is, V decays with almost a 100% branching ratio into $\chi_1\chi_2$ while direct $V \to e^+e^-$ ($\mu^+\mu^-$) decays are suppressed as ε^2 and thus subdominant. The $\chi_2 \to \chi_1$ (hadrons) decay will also be present at a similar level than the (semi)leptonic channels (see e.g. figure 1 of [58]). As argued in section 2.3, due to the fact that the SM hadronic cross section is much larger than the leptonic ones, the relative NP correction to the hadronic channel will be accordingly suppressed. For this reason we will not include it in our simulations.

The lightest new fermion χ_1, which may play the role of the dark matter particle, is stable and escapes undetected, while the heavier fermion χ_2 decays into $\chi_1\,e^+e^-$ ($\mu^+\mu^-$), providing the main contribution to the NP-related additional electron-positron (di-muon) pairs. The V width that is almost saturated by the $V \to \chi_1\chi_2$ process will be an important quantity in the rest of this work. In the limit $\delta m = m_V - (m_{\chi_1} + m_{\chi_2}) \ll m_V$ we have:

$$\Gamma_V \simeq \frac{2\alpha_D \sqrt{\delta m}(\delta m + 2m_{\chi_1})^{3/2}}{m_V} \,. \tag{3.11}$$

In particular, in the benchmark points used in the next section, phase space suppression due to $m_{\chi_2} \sim m_V$ leads to a width of order MeV. Note that since there are charged particles in the decay chain final state, the V boson escapes invisible decays searches. At the same time, since the three body decay $\chi_2 \to \chi_1 e^+e^-$ is characterised by a continuous and smooth e^+e^- energy spectrum, it also escapes standard "bump" searches.

The mass of the dark Higgs boson depends on its quartic coupling λ_S, which is a free parameter in the theory. The particular case $m_S \lesssim 2m_{\chi_1}$, which ensures that the $S \to \chi_1\chi_1$ decay channel is closed, represents an interesting possibility to render χ_1 a good DM candidate [59–61]. The argument proceeds in two steps:

1. The t-channel p-wave $\chi_1\chi_1 \leftrightarrow SS$ process is enhanced by a relatively large Yukawa coupling (see eq. (3.8)). As a consequence, it keeps χ_1 in equilibrium with the S population up to a temperature T_{fo}. This temperature can be modified by changing the S mass in the regime $m_S \gtrsim m_{\chi_1}$.

2 At $T \gtrsim m_S$ thermal equilibrium between the dark sector composed of S and χ_1 and the lightest SM particles is typically maintained via the standard $\chi_2\chi_1 \to e^+e^-$ process, with the χ_1 relativistic. Moreover, at $T < m_S$, the contribution of S decays and

JHEP06(2022)122

inverse decays mediated by a triangle loop involving VVe maintains S in thermal equilibrium.[5] Consequently, S continues to be coupled to the thermal bath down to temperatures $T \ll m_S$ and in particular throughout the $\chi_1\chi_1 \to SS$ annihilation process.

Arranging for freezing-out the $\chi_1\chi_1 \to SS$ process around $T_{\rm fo} \sim m_{\chi_1}/20$ then allows to reproduce the correct dark matter relic density. This corresponds to the "forbidden annihilation" regime of the iDM model which can be realised when $\frac{M_S}{2} \lesssim m_{\chi_1} \lesssim M_S$.[6]

Finally, let us briefly discuss the direct contribution of V to the muon $g-2$. Any vector particle with a direct interaction with muons will give rise to a one-loop contribution to a_μ. For a pure vector coupling, this contribution can be written as:

$$\Delta a_\mu = \frac{\alpha_{\rm em}\varepsilon^2}{2\pi}\, x_\mu^2\, \mathcal{F}\left(x_\mu\right) , \tag{3.12}$$

where $x_\mu = m_\mu/m_V$, $g_{eV} = \varepsilon e$ with e the electromagnetic coupling constant, and the loop function $\mathcal{F}$ is given by:

$$\mathcal{F}(x) = \int_0^1 dz\, \frac{2z^2\,(1-z)}{x^2 z + (1-z)(1-x^2 z)} . \tag{3.13}$$

For m_V in the GeV range, the loop function simplifies and one has approximately

$$\Delta a_\mu \sim 2\cdot 10^{-9} \times \left(\frac{e\varepsilon}{0.005}\right)^2 \times \left(\frac{1\,\text{GeV}}{m_V}\right)^2 . \tag{3.14}$$

The direct contribution in eq. (3.14), together with the indirect corrections from the luminosity determination, can reconcile the theoretical predictions for a_μ with the experimental results.

3.2 Numerical analysis: luminosity determination

We have implemented the iDM model in FeynRules/UFO [65–67] files, and we have used the MadGraph5_aMC@NLO platform [68] in order to generate s- and t-channel e^+e^- events[7] that would contribute to the KLOE, BaBar and BESIII measurements of the Bhabha cross section.[8] We have simulated the process $e^+e^- \to \chi_1\chi_1 e^+e^-$ and we have applied the relevant cuts directly on the generated final states. For the luminosity measurement, the different experiments exploited various kinematic ranges:

[5] Note that these loop processes typically dominate over the Higgs-portal induced interactions due to the large kinetic mixing considered in this study (see e.g. [59]).

[6] In the case where the S boson has a longer life-time, additional effects such as the dilution of the χ_1 relic density from the entropy injection from $S \to e^+e^-$ could also lead to the proper relic density, see the recent work [62], although additional constraints from BBN then apply (see e.g. [59, 63, 64].

[7] We simulate $e^+e^- \to \chi_1\chi_2, \chi_2 \to \chi_1 e^+e^-$, including the leptonic branching ratios of the χ_2.

[8] The two experiments CMD-2 [26, 69] and SND [29, 70] carried out measurements in the energy range for $\pi^+\pi^-(\gamma)$ production by scanning directly with the beam energy. For each point, Bhabha events were used to calibrate the luminosity. The angular cuts applied are respectively $\cos\theta \in [-0.83, 0.83]$ (SND [70]) and $\cos\theta \in [-0.45, 0.45]$ (CMD-2 [26]) . These experiments differ in two main aspects from the previous ones. First they cannot distinguish easily π's from μ's, so that the final hadronic cross-section can be obtained only after subtracting the $e^+e^- \to \mu^+\mu^-$ component by relying on the theoretical estimation. Second, each energy point in the scan has its own luminosity measurement, so that the effects of NP would need to be estimated independently for each $\sqrt{s}$.

JHEP06(2022)122

- At KLOE, with CoM energy $\sqrt{s} = 1.02\,\text{GeV}$, the following cuts were applied [71]: $\cos\theta \in [-0.57, 0.57]$, $E_e \in [0.3, 0.8]\,\text{GeV}$, $p \geq 400\,\text{MeV}$ and a cut on the polar angle acollinearity $\zeta < 9°$. KLOE reported the Bhabha cross section $\sigma^{\text{vis}}_{e^+e^-} = (431 \pm 0.3)\,\text{nb}$.

- At BaBar, with asymmetric collisions of 9 GeV electrons and 3.1 GeV positrons corresponding to $\sqrt{s} = 10.58\,\text{GeV}$, the following cuts were applied [72]: the polar angles in the centre of mass are required to satisfy $|\cos\theta| < 0.7$ for one track and $|\cos\theta| < 0.65$ for the other; the scaled momentum $P_i = 2p_i/\sqrt{s}$, where p_i are the momenta of the track i and $\sqrt{s}$ is the CoM energy, were required to satisfy $P_1 > 0.75$ and $P_2 > 0.5$ ($i = 1$ denotes the track with the higher CoM momentum); the cut on the acollinearity angle was $\zeta < 30°$. The luminosity was estimated also by exploiting the $e^+e^- \to \mu^+\mu^-$ process and, according to the uncertainties reported in table 3 of [72], the muon process slightly dominates the average. Furthermore, BaBar associated a 0.7% uncertainty on the Bhabha estimates due to "Data-MC differences". After accounting for the detector efficiency, the reported measurement for the Bhabha cross section is $\sigma^{\text{vis}}_{e^+e^-\to e^+e^-} = (6.169 \pm 0.041)\,\text{nb}$ and that for the $e^+e^- \to \mu^+\mu^-$ process is $\sigma^{\text{vis}}_{e^+e^-\to\mu^+\mu^-} = (0.4294 \pm 0.0023)\,\text{nb}$.

- The BESIII collaboration also delivered an initial state radiation (ISR) measurement [30], although with larger uncertainties, at the CoM energy $\sqrt{s} = 3.773\,\text{GeV}$. This measurement is in better agreement with KLOE data. The luminosity estimate [73] relies solely on Bhabha scattering, with the relatively loose cuts $\cos\theta \in [-0.83, 0.83]$. They reported a Bhabha cross section of $\sigma^{\text{vis}}_{e^+e^-} = (147.96 \pm 0.74)\,\text{nb}$.

Because of the strong suppression of the Bhabha scattering due to the angular cuts and the ε^4 suppression of direct leptonic V decays, the order percent NP contribution required to shift significantly a_μ^{HVP} cannot be obtained from the off-shell exchange of a V boson. However, for s-channel on-shell V production the suppression is partly compensated by the resonant nature of the process. The direct consequence is that given a vector boson V of a certain mass, at most one among the above experiments can be affected non-negligibly in its luminosity determination.

Since the KLOE measurement is the main responsible of reducing the data driven value of the HVP, we need to increase σ_{had} around the CoM energy of $\sim 1\,\text{GeV}$. Accordingly, we require a dark photon mass $m_V \sim 1\,\text{GeV}$. In this case NP effects on the luminosity measurement will translate into a large contribution to the hadronic cross section as derived from the KLOE data. On the other hand, for the other experiments the corresponding effects are off-resonance, and we have explicitly checked that they are negligible for the relevant parameter space of our model. Figure 2 shows the relative enhancement δ_R of eq. (2.6) of the inferred Bhabha cross section as a function of the mass of the dark photon. This directly translates into an equal enhancement of the hadronic cross section. The dashed curves are obtained for $m_{\chi_2} = 0.90\,m_V$, while the solid curves for $m_{\chi_2} = 0.93\,m_V$. The different colors denote different values of the dark coupling $\alpha_D = 0.05$ (blue), 0.1 (yellow) and 0.5 (green). In addition, we fixed $m_{\chi_1} = 18\,\text{MeV}$ and the dark photon couplings to electrons and muons to $\varepsilon\, e = 5 \times 10^{-3}$. As we will discuss in section 4, this value for the couplings is allowed

JHEP06(2022)122

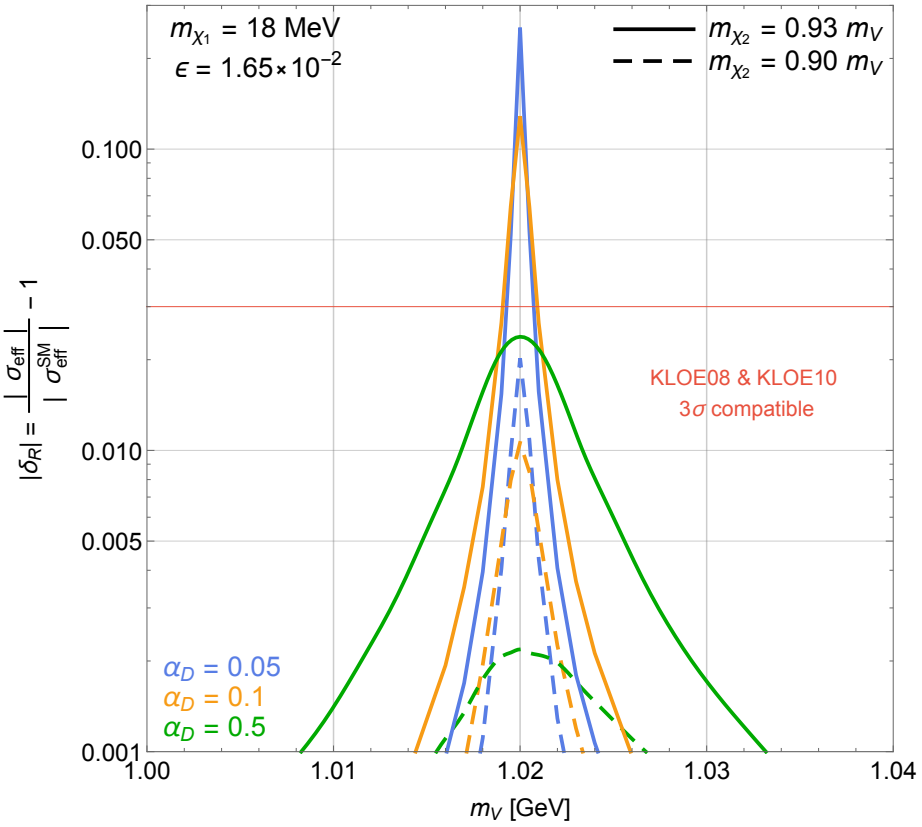

Figure 2. Relative enhancement δ_R of the inferred Bhabha cross section as a function of m_V for $m_{\chi_2} = 0.93\, m_V$ (solid curves) and $m_{\chi_2} = 0.9\, m_V$ (dashed curves), and $\alpha_D = 0.05$ (blue), 0.1 (orange) and 0.5 (green). In this plot $m_{\chi_1} = 18\,\text{MeV}$ and $\varepsilon = 1.65 \times 10^{-2}$. Below the red horizontal line all the KLOE measurements are consistent at a 3σ level.

by current experimental results. The red horizontal line indicates the value of δ_R below which KLOE08 and KLOE12 remain compatible within 3σ with KLOE10. In this region, all other measurements also agree with the combined KLOE result at better than 3σ.

3.3 Numerical analysis: the $\sigma(\mu\mu\gamma)$ method

New physics strongly modifies the $\mu\mu\gamma$ cross-section without need of tuning m_V around the experimental CoM energy. This is due to the fact that the $\mu\mu\gamma$ cross-section is smaller than the Bhabha one. The experimental cuts are as follow:

- KLOE12 [36] analysis relied on a final state with a *missing photon*, with the kinematic cuts on the muons $\cos\theta_\mu \in [-0.64, 0.64]$, and $p_{\mu T} \geq 160\,\text{MeV}$ or $p_{z\mu} \geq 90\,\text{MeV}$ and a cut on the (assumed) polar angle of the missing photon (reconstructed from the muons momenta) $\cos\theta_\gamma > 15^o$. Finally, the reconstructed track mass m_{tr} of each μ, as defined in [36] must satisfy $m_{tr} \subset [0.08, 0.115]$ to distinguish them from pions.

- BESIII [30] analysis uses a final with a *visible* photon, with $|\cos\theta_\gamma| < 0.93$ and $E_\gamma = 0.4\,\text{GeV}$. Both muons are required to have $\cos\theta_\mu \in [-0.92, 0.92]$, and $p_{\mu T} \geq 300\,\text{MeV}$. An additional criterium of consistency of the final states with a $\mu\mu\gamma$ is implemented via

JHEP06(2022)122

the so-called $4C$ kinematical fit. The latter cannot be straightforwardly reproduced, we note however that the cut on χ^2 used in [36] $\chi^2 < 60$ is relatively loose. Accounting for the energy resolution of 2.5%, we required the missing energy in the system to be smaller than 0.3 GeV. Note that tightening this requirement to 0.2 GeV reduces the NP contribution by three.

- At BaBar [37], both visible and invisible channels where used and the analysis is significantly more involved. In view of the importance of properly implementing the experimental cuts in the two previous experiments, we leave for future work a complete simulation of the BaBar measurement.

We have used the same approach than for the Bhabha cross-section, relying on the MadGraph5_aMC@NLO platform [68] to simulate the NP contributions. In the KLOE12 [36] case, the relevant process is $e^+e^- \to \chi_1\chi_2$ via the resonant V production. In BESIII, we instead produced directly the V in addition to the hard photon $e^+e^- \to V\gamma$, closely mimicking the SM ISR process. In both cases, the NP does not include soft or collinear photons (since a hard photon is required for BESIII) and is performed at leading order in QED. In both cases, the amount of missing energy in our final states determines the efficiency of the experimental cuts. In term of our iDM model, the mass m_{χ_1} of the dark matter candidate has a strong influence on the final result, with smaller values leading to stronger effects.

We show in figure 3 the resulting shift for a parameter point chosen for simplicity such that the relative shift in KLOE12 (denoted by $\delta_\mu^{\text{KLOE12}}$), BESIII ($\delta_\mu^{\text{BESIII}}$) and in KLOE08 ($\delta_R$) are of the same order. We also include three curves depicting different guesses for the effect in BaBar (solid black: $\delta_\mu^{\text{BaBar}} = 0$, dashed gray: $\delta_\mu^{\text{BaBar}} = \delta_\mu^{\text{BESIII}}/2$, dot-dashed gray: $\delta_\mu^{\text{BaBar}} = \delta_\mu^{\text{BESIII}}$). The dotted green curve shows the combined KLOE result. In all cases, above the dotted purple horizontal line, agreement between the data-driven approach and the BMW lattice result is achieved with 90% C.L.. Yet, the overall effect of the indirect corrections does not suffice to provide a complete solution to the Δa_μ anomaly eq. (1.1).

Let us close this section by pointing that each of the effects described above requires a different degrees of tuning on the parameters of our model. The shift from $\sigma(\mu\mu\gamma)$ method with a visible γ like in the analysis of ref. [30] does not require any particular tuning, and will thus be affected in any iDM model with sufficiently large kinetic coupling ε. (This can be seen from the constant value reached by $a_\mu^{\text{LO,HVP}}$ in figure 3 when the KLOE CoM does not correspond precisely to m_V.) The effect on KLOE12 that exploits the $\sigma(\mu\mu\gamma)$ method where the photon is not detected requires $m_V \sim m_\phi$, but does not depends critically on the value of m_{χ_2}. Finally, the luminosity method used by KLOE08 requires both $m_V \sim m_\phi$ and $m_{\chi_2} \lesssim m_V$.

4 Relevant constraints

In this section we study the most relevant constraints on the iDM scenario outlined in section 3.1.

JHEP06(2022)122

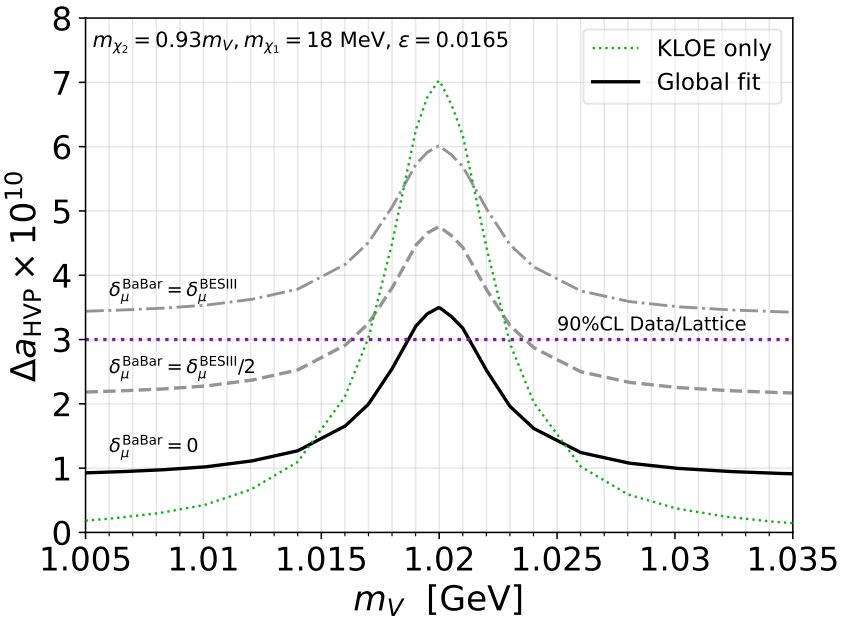

Figure 3. Theoretical prediction for the shift in $a_\mu^{\rm LO,HVP}$ as a function of m_V for a dark photon model with $m_{\chi_1} = 18\,\text{MeV}$, $m_{\chi_2} = 0.93\,m_V$, $\alpha_D = 0.5$ and $\epsilon = 0.0165$, which leads to $\delta_\mu^{\rm KLOE12} \sim \delta_\mu^{\rm BESIII}$. The dotted green line shows the combined KLOE result, while the thick black curve includes all the measurements, assuming negligible shifts on BaBar results. The dashed grey lines indicate the effect of an hypothetical shift in BaBar $\delta_\mu^{\rm BaBar} = \delta_\mu^{\rm BESIII}$ (top) and $\delta_\mu^{\rm BaBar} = \delta_\mu^{\rm BESIII}/2$ (bottom). Above the dashed purple line the BMW lattice result and the data-driven analysis agree at better than the 90% C.L.

4.1 BaBar dark photon searches

The BaBar experiment made two searches relevant to our case. The first one focuses on resonances in the e^+e^- spectrum with an energetic initial state radiation (ISR) photon [74]. They applied the following selection cuts (with all variables in the CoM frame): $\cos\theta_{e^+} > -0.5$, $\cos\theta_{e^-} < 0.5$, $E_\gamma > 0.2\,\text{GeV}$ and $E_\gamma + E_{e^+} + E_{e^-} \simeq 10.58\,\text{GeV}$.

The polar angles are defined with respect to the electron beam direction, and the last selection cut requires the centre-of-mass energy of the candidate event to be within the beam energy spread, that is around 5–10 MeV [75] (see also [76], which quotes the spread 5.5 (2.7) MeV for the e^- (e^+) beam). This search is ineffective in constraining the iDM model because the emission of two χ_1 states always results in missing energy larger than 20 MeV, that is larger than the beam energy spread.

In the second search, BaBar analysed single photon events with large missing energy searching for bumps in the photon spectrum [77] (which superseded the older search for invisible final states in single-photon decays employed in $\Upsilon(1S)$ [78]). We reinterpret the mono-photon sensitivity exploiting the same strategy of [79–81]. Since this search does not use cuts on simple quantities but a multivariate analysis, we use the following cuts: the events satisfy the mono-photon selection criteria if $E^\gamma_{\rm CMS} > 2\,\text{GeV}$, $-0.16 \lesssim \cos(\theta_\gamma) \lesssim 0.84$ and $p(e^-) < 150\,\text{MeV}$ or $p(e^+) < 150\,\text{MeV}$. The expected sensitivity in terms of the kinetic

JHEP06(2022)122

mixing $\varepsilon = g_{eV}/e$ for the iDM model is obtained as [80]

$$\varepsilon_{\rm exp}^{\rm iDM} = \varepsilon_{\rm exp}^{\rm mono-\gamma}\sqrt{\frac{N_{\gamma\ \rm cuts}}{N_{\rm all}}}\,, \tag{4.1}$$

where $\varepsilon_{\rm exp}^{\rm mono-\gamma}$ is the current bound from the BaBar mono-photon analysis [77], $N_{\gamma\ \rm cuts}$ are the number of events selected using only the photon cuts, and $N_{\rm all}$ are the number of events that pass all the cuts.

Although BaBar results do not constrain significantly our scenario, the semi-visible final states could be probed in the future by Belle-II [80, 82], possibly from longer decay chain involving also the dark Higgs boson [83]. One key factor compared to the analysis in ref. [80] is that here we are concerned with a parameter space region in which the V decay does not lead to a displaced vertex. A complete background study is thus required to derive a proper projection of the foreseeable constraints on our scenario.

4.2 Effects on the ϕ-meson properties

Since the dark photon mass must be close to the KLOE CoM energy, it will also be close to the ϕ-meson mass, and thus the two widths Γ_ϕ and Γ_V will overlap, possibly affecting the properties of the ϕ. In particular, if the dark photon couples universally to all SM fermions proportionally to their electric charge, then its coupling to the strange quark will unavoidably induce $\phi - V$ mixing (instead, in the case of a more specific lepto-philic vector boson, this would not occur, and the analysis below would not apply).

The mixed mass term $M_{V\phi}$ can be derived from the real part of the off-diagonal self-energy of the (V, ϕ) system. Assuming $m_V \sim m_\phi$ we have

$$M_{V\phi} = \frac{1}{2m_\phi}\langle V|\frac{e\varepsilon}{3}V_\rho \bar{s}\gamma^\rho s|\phi\rangle \tag{4.2}$$

$$= f_\phi \frac{e\varepsilon}{6} \sim 0.25\,\text{MeV} \times \left(\frac{\varepsilon}{0.01}\right)\,, \tag{4.3}$$

where f_ϕ is the ϕ meson decay constant defined as

$$\langle 0|\bar{s}\gamma^\rho s|\phi\rangle = f_\phi m_\phi \epsilon^{*\,\rho}\,,$$

and we have factorised the amplitude and used the fact that mixing can only occur between states with the same polarisation ϵ^*. The evolution in time of the mixed states is governed by the time-dependent Heisenberg equation:

$$i\frac{\partial}{\partial t}\begin{pmatrix}|\phi\rangle\\ |V\rangle\end{pmatrix} = \begin{pmatrix} m_\phi - i\frac{\Gamma_\phi}{2} & M_{V\phi}\\ M_{V\phi} & m_V - i\frac{\Gamma_V}{2}\end{pmatrix}\begin{pmatrix}|\phi\rangle\\ |V\rangle\end{pmatrix}\,. \tag{4.4}$$

Mixing effects are strongly suppressed when the diagonal entries in the effective Hamiltonian differ sizeably, that is when $|m_\phi - m_V| \gg M_{V\phi}$ or $|\Gamma_\phi - \Gamma_V| \gg M_{V\phi}$. For instance, in the case $m_V \simeq m_\phi$ but $\Gamma_V \neq \Gamma_\phi$, the mass difference $m_{\chi_2} - m_{\chi_1}$ between the two mass eigenstates is given by

$$m_{\chi_2} - m_{\chi_1} = \frac{2\pi\alpha_{\rm em}(m_\phi - m_V)\varepsilon^2 f_\phi^2}{9(\Gamma_V - \Gamma_\phi)^2}\,. \tag{4.5}$$

JHEP06(2022)122

For the range of parameters relevant for this work, the mass shift is both smaller than the experimental uncertainty on the ϕ mass ($m_\phi^{\rm exp} = 1019.461 \pm 0.016\,\text{MeV}$) and orders of magnitude lower than the uncertainty on the lattice prediction ($m_\phi^{\rm th} = 1018 \pm 17\,\text{MeV}$ [84]).[9] Similarly, the shifts in the width of the mass eigenstates are safely suppressed by ε^2.

Another point that we need to check concerns the partial width for ϕ decays into leptons, that is strongly suppressed with respect to hadronic decay channels, and which could be affected by mixing with the V. The experimental value is $\Gamma_{\phi ee}^{\rm exp} = 1.27 \pm 0.04\,\text{keV}$ [85] while recent QCD lattice estimate have a theoretical errors of the same order, dominated by the theoretical error on the ϕ meson decay constant $f_\phi = 241 \pm 9 \pm 2\,\text{MeV}$ [84]. It is straightforward to solve numerically eq. (4.4) and derive the time-dependent evolution of the mixed states: $|\phi(t)\rangle = a(t)|\phi\rangle + b(t)|V\rangle$, where the kets in the right-hand side corresponds to the states at $t = 0$. Since both the mixing term b and the V decay width in e^+e^- are ε-suppressed, the dominant modification to the ϕ leptonic width will arise from the time-integration of the $|a(t)|$ factor. By taking $m_V \simeq m_\phi$ and $\Gamma_V \neq \Gamma_\phi$ the change in the leptonic width is well reproduced by the following scaling

$$\frac{|\delta\Gamma_{\phi ee}|}{\Gamma_{\phi ee}} \sim \varepsilon^2 \frac{f_\phi}{|\Gamma_\phi - \Gamma_V|}\,. \tag{4.6}$$

For all relevant points in our parameter space, this correction remains safely below the experimental and theoretical uncertainties which are both of a few percent.[10]

Altogether, we can conclude that both the measurements and the theoretical predictions for ϕ-meson related observables do not have a sufficient level of precision to constrain effectively our NP scenario. Eventually, the main reason underlying this conclusion is that both the ϕ and the V boson have very suppressed leptonic branching ratios, while their main decay channels $\phi \to$ hadrons and $V \to \chi_1\chi_2$ are completely different final states.

4.3 KLOE10 off-resonance measurement

The second analysis from the KLOE collaboration, KLOE10 [42], was performed $\sim 20\,\text{MeV}$ below the ϕ resonance, at $\sqrt{s} = 1.00\,\text{GeV}$. This implies that if the V width is significantly smaller than 20 MeV, KLOE08 [35] and KLOE10 [42] measurements cannot be simultaneously shifted by similar amounts. A naive comparison indicates that the two measurements would remain in agreement at the 2σ level if the shift does not exceed $\delta_R \simeq 2\%$. However, the final KLOE result is in fact a simultaneous fit to three analysis (including the last KLOE12 [36]) which was carried out by the KLOE collaboration in ref. [24]. The combined KLOE result takes into account sizeable correlations between various systematic uncertainties which dominate the overall error, and which increase it by about 60% with respect to

[9] The mixing is maximal when $m_V = m_\phi$ and $\Gamma_V = \Gamma_\phi$, in which case the mass splitting is simply $\delta m = 2M_{V\phi}$. This shift is still an order of magnitude lower than the theoretical estimate for m_ϕ [84] so that we cannot derive useful constraints from the mass shift. Note that the splitting is also smaller than Γ_ϕ, so that at KLOE both ϕ and V can be simultaneously produced on resonance.

[10] We have cross-checked numerically this result by adding also the direct $V \to e^+e^-$ contribution. In this case both the $\phi \to e^+e^-$ and $V \to e^+e^-$ amplitudes must be estimated and their interference must be included in the time-integrated decay rate. We have found that the correction saturates the experimental uncertainty only for rather large values of kinetic mixing, exceeding ~ 0.05.

JHEP06(2022)122

a naive estimate assuming uncorrelated measurements.[11] Systematic correlations might thus allow for somewhat larger values of δ_R while maintaining compatibility between the different results, and for this reason we relax the compatibility requirement to

$$\delta_R \lesssim 2.5\% \quad \text{when } \Gamma_V \ll 20 \text{ MeV}\,. \tag{4.7}$$

In our benchmark iDM scenario, the V width is typically of the order of few MeVs, making this constraint relevant. However, this is still a large enough shift to solve the tension with the BaBar result.

4.4 Muon cross-section measurements

The KLOE [36], BaBar [37] and BESIII [30] collaborations have also measured $\mu\mu\gamma$ final states to determine the differential luminosity by comparing with the theoretical $\sigma_{\mu\mu} \equiv \sigma(e^+e^- \to \mu^+\mu^-\gamma)$ cross-section, and cross-checked the results with the total luminosity as determined from Bhabha scattering. Agreement is usually obtained at or below the percent level for the overall integrated cross-sections. However, for specific subsets of di-muon invariant mass bins deviations can be significant (see e.g. the data in the $m^2_{\mu\mu} \sim (0.6\text{–}0.9)\,\text{GeV}^2$ windows reported in figure 5 in ref. [36], figure 32 in ref. [37] and figure 1 in ref. [30]). We will focus here on the analysis of the KLOE collaboration [36] (KLOE12) which exploits $\mu\mu\gamma$ final states in which the γ is not reconstructed. Assuming that the branching fractions for V boson decays into muons and electrons are similar, as would be implied by universality of the V couplings to leptons, we would expect a relative excess of di-muon events similar to the excess of e^+e^- Bhabha events in the KLOE08 measurement [35]. KLOE12 further observed that the integrated $\mu\mu\gamma$ cross-section was in accordance with the theoretical prediction up to a $\sim 1\%$ systematic uncertainty. Since this measurement relied on the same method to estimate the luminosity [71] as the KLOE08 analysis, in reconstructing the cross-section the direct contribution to $\mu\mu$ events from $\mu^+\mu^-(\chi_1\chi_1)$ can be compensated at least in part by the effect of overestimating the luminosity because of a similar excess of $e^+e^-(\chi_1\chi_1)$ Bhabha events. In fact, let us consider figure 5 in ref. [36] where the number of $\mu\mu\gamma$ events expected in the SM $N^{\text{SM}}_{\mu\mu}$ was estimated with the Phokhara MC, and compared to the experimental data $N^{\text{exp}}_{\mu\mu}$. From the QED cross-section $\sigma_{\mu\mu}$ one estimates

$$N^{\text{SM}}_{\mu\mu} = \epsilon^{\text{SM}}_{\mu}\sigma_{\mu\mu} \times \mathcal{L}^{\text{SM}}_{e^+e^-} \tag{4.8}$$

where $\epsilon^{\text{SM}}_{\mu}$ is the experimental efficiency for the SM signal and $\mathcal{L}^{\text{SM}}_{e^+e^-} = \mathcal{L}_{e^+e^-}(1+\delta_R)$ is the (overestimated) luminosity inferred by assuming only QED Bhabha scattering, while $\mathcal{L}_{e^+e^-}$ is the true luminosity obtained after accounting for the NP contribution δ_R to e^+e^- events, see eq. (2.5) in section 2.2. On the other hand, the experimental data include also a direct NP contribution $\sigma^{\text{NP}}_{\mu\mu X}$ from $\mu^+\mu^-(\chi_1\chi_1)$ events mimicking $\mu\mu\gamma$ final states with an undetected γ, and measured with efficiency $\epsilon^{\text{NP}}_{\mu}$, so that

$$N^{\text{exp}}_{\mu\mu} = \left(\epsilon^{\text{SM}}_{\mu}\sigma_{\mu\mu} + \epsilon^{\text{NP}}_{\mu}\sigma^{\text{NP}}_{\mu\mu X}\right) \times \mathcal{L}_{e^+e^-} = \epsilon^{\text{SM}}_{\mu}\sigma_{\mu\mu}\,(1+\delta_\mu) \times \mathcal{L}_{e^+e^-}\,. \tag{4.9}$$

[11] KLOE08 and KLOE12 have also a fully correlated statistical error, since are based on the same dataset. Statistical errors are, however, a subdominant source of uncertainty.

JHEP06(2022)122

All in all, from equations (4.8) and (4.9), we obtain:

$$\frac{N_{\mu\mu}^{\rm exp}}{N_{\mu\mu}^{\rm SM}} = \frac{1+\delta_\mu}{1+\delta_R}\,, \tag{4.10}$$

which shows how the direct effect δ_μ and the indirect (luminosity-related) effect δ_R tend to compensate in the ratio. Note, however, that while the relative luminosity shift δ_R defined in section 2.2 is independent of the CoM energy of the e^+e^- collision, that is, it remains constant with respect to the reconstructed di-muon invariant mass squared s', this is not true for the direct effect. This depends on the different energy behaviour of the SM and NP cross sections, so that we have as in eq. (2.10):

$$\delta_\mu(s') = \frac{\sigma_{\mu\mu X}^{\rm NP}(s')}{\sigma_{\mu\mu}(s')}\frac{\epsilon^{\rm NP}}{\epsilon^{\rm SM}}\,, \tag{4.11}$$

with the experimental efficiencies explicitly included for clarity. As a consequence of the s' dependence in δ_μ, also the ratio in eq. (4.10) will depend on s'.

In order to numerically estimate the predicted ratio $N_{\mu\mu}^{\rm exp}/N_{\mu\mu}^{\rm SM}$ with the NP effects included, we have implemented in the MadGraph5_aMC@NLO platform [68] the $e^+e^- \to \mu^+\mu^-\chi_1\chi_1$ process along with the cuts described in ref. [36]. In particular, at KLOE the identification of $\mu^\pm$ (and $\pi^\pm$) events relies on the "computed track mass" m_{tr}, which is defined in terms the momentum p_+ and p_- of the reconstructed positively and negatively charged tracks, and of the missing energy of the event, as the solution of energy conservation. Under the assumption that the missing energy is carried away by a photon we have $E_\gamma^2 = |\vec{p}_\gamma|^2 = |\vec{p}_- + \vec{p}_+|^2$, and the energy conservation condition reads

$$\left(\sqrt{s} - \sqrt{|\vec{p}_+|^2 + m_{tr}^2} - \sqrt{|\vec{p}_-|^2 + m_{tr}^2}\right)^2 - |\vec{p}_- + \vec{p}_+|^2 = 0\,. \tag{4.12}$$

For muon identification it is required that the solution satisfies $80 \le m_{tr}/\text{MeV} \le 115$. However, for $\mu^+\mu^-(\chi_1\chi_1')$ final states energy conservation would imply the replacement $|\vec{p}_- + \vec{p}_+|^2 \to (E_{\chi_1} + E_{\chi_1'})^2$ so that if eq. (4.12) is instead still used, one tends to obtain track mass solutions that are somewhat larger than the muon mass (with values that depend on M_{χ_1}), so that certain $\mu^+\mu^-$ events do not pass the m_{tr} cut and are rejected. However, the most important suppression of the number of $\mu^+\mu^-(\chi_1\chi_1')$ events that pass the cuts arises from the requirement that the polar angle $\theta_{\mu\mu}$ of the di-muon momentum $\vec{P}_{\mu\mu} = \vec{p}_+ + \vec{p}_-$ satisfies $\cos\theta_{\mu\mu} > \cos 15°$.[12] It is thus clear that if we assume that $\chi_1\chi_1'$ are emitted approximately isotropically, the momentum of the recoiling di-muon system will pass this cut only a fraction $(\sin 15°)^2/2 \sim 3.5\%$ of the times.

We illustrate the results of our simulation in figure 4. The slope of the ratio is generated by the $\delta_\mu(s')$ correction and is mostly active at small values of s', where the SM $\mu\mu\gamma$ signal is more suppressed. The luminosity effect instead shifts the entire curve downwards. All in all, we have estimated the χ^2 value for the green curve in figure 4, and we have found

[12] This cut selects recoiling photons that are emitted at small angles with respect to the beam direction, which largely enhances the number of ISR with respect to FSR γ events.

JHEP06(2022)122

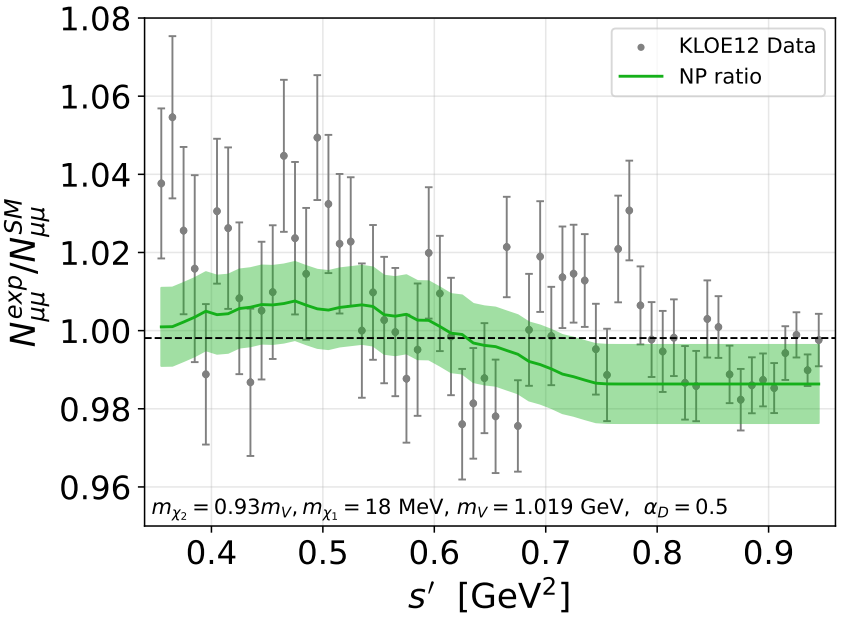

Figure 4. New physics contributions on the ratio $N_{\mu\mu}^{\rm exp}/N_{\mu\mu}^{\rm SM}$ for our iDM model with $m_{\chi_2} = 0.95\,\text{GeV}, m_{\chi_1} = 18\,\text{MeV}$ and $\varepsilon = 0.013$ (green line). The grey points are the KLOE data [36] and the black line the data fit to a constant ratio. We have added a 1% uncertainty corresponding to the experimental systematics for visualisation [36].

that it yields a value roughly similar to the χ^2 of the constant fit.[13] However, the NP effect has the interesting feature of being able to better accommodate, at least qualitatively, the behaviour of the data, which at small s' overshoot the constant fit, while for large s' undershoot it.

4.5 KLOE forward-backward asymmetry

The KLOE collaboration performed an analysis of the forward-backward asymmetry $A_{\rm FB}$ in $e^+e^- \to e^+e^-$ around the ϕ resonance in order to extract the leptonic widths $\Gamma_{\phi ee}$ and $\Gamma_{\phi\mu\mu}$ and to carry out a test of lepton flavour universality [43]. They measured $A_{\rm FB}$ for three different CoM energies:

$$A_{\rm FB}(\sqrt{s}) = \begin{cases} 0.6275 \pm 0.0003 & (\sqrt{s} = 1017.17\,\text{MeV} \simeq m_\phi - \Gamma_\phi/2) \\ 0.6205 \pm 0.0003 & (\sqrt{s} = 1019.72\,\text{MeV} \simeq m_\phi) \\ 0.6161 \pm 0.0004 & (\sqrt{s} = 1022.17\,\text{MeV} \simeq m_\phi + \Gamma_\phi/2)\,, \end{cases} \tag{4.13}$$

where all three data-points share a common systematic uncertainty of 0.002. The collaboration then fitted these three experimental values to the interference pattern expected from the ϕ to obtain the measurement $\Gamma_{\phi ee} = 1.32 \pm 0.05 \pm 0.03\,\text{keV}$. An off-shell V exchange will also induce an interference pattern in the asymmetry, we can re-interpret this measurement as being a limit on the V contribution. However, we also must include the

[13] A more recent dataset on muonic events with similar errors was presented in ref. [86].

JHEP06(2022)122

direct contribution from the $e^+e^- \to V \to \chi_1\chi_1 e^+e^-$ process. Let us denote the measured number of forward/backward events as N_F and N_B. The asymmetry can be decomposed as

$$A_{\rm FB}(\sqrt{s}) \equiv \frac{N_F - N_B}{N_F + N_B} \tag{4.14}$$

$$= A_{\rm FB}^{\rm Bhabha} \times (1 - \delta_R(\sqrt{s})) + A_{\rm FB}^{\phi} + A_{\rm FB}^{V}\,. \tag{4.15}$$

The first term of the second line includes a correction which is due to the fact that the process $e^+e^- \to V \to \chi_1\chi_1 e^+e^-$ contributes to the denominator of the Bhabha asymmetry while, since it has a negligible asymmetry, it does not contribute to the numerator. The second and third contributions correspond to the interference between virtual photon exchange and respectively the ϕ and the V vector boson. Since the V is produced resonantly, the correction δ_R depends strongly on $\sqrt{s}$ and on the value of the V width. The effect of δ_R is to reduce the asymmetry, while both the interference terms contribute positively.

In order to assess the complete V contribution, we have simulated the full process $e^+e^- \to e^+e^-$ in MadGraph5_aMC@NLO, implementing the cuts given in [43]. It is clear that the fit performed by the collaboration cannot be applied to the scenario at hand with multiple interference terms plus the "inverse resonance" effect. Hence we instead adopt a more conservative proxy, the difference between the lowest and the highest measurements of $A_{\rm FB}$ in $\sqrt{s}$:

$$\Delta A_{\rm FB} \equiv \frac{A_{\rm FB}(m_\phi - \Gamma_\phi/2) - A_{\rm FB}(m_\phi + \Gamma_\phi/2)}{A_{\rm FB}(m_\phi - \Gamma_\phi/2) + A_{\rm FB}(m_\phi + \Gamma_\phi/2} \tag{4.16}$$

$$= \Delta A_{\rm FB}^{\phi} + \Delta A_{\rm FB}^{V} - \frac{\delta_R(\sqrt{s_-}) - \delta_R(\sqrt{s_+})}{2}\,, \tag{4.17}$$

where $s_\pm \simeq m_\phi \pm \Gamma_\phi/2$ are the CoM energies of the KLOE measurements, cf. eq. (4.13). KLOE measured $\Delta A_{\rm FB}^{\rm exp} = (9.17 \pm 0.35) \cdot 10^{-3}$. In either the vector meson dominance[14] or in a simple factorisation approach, the ϕ-mediated interference cross-section can be obtained as

$$\sigma_{\rm int} = \frac{3\alpha_{\rm em}\Gamma_{\phi ee}}{m_\phi} \frac{s - m_\phi^2}{(s - m_\phi^2)^2 + s\Gamma_\phi^2} \int_{c_{\rm min}}^{c_{\rm max}} dc_\theta \left[\pi\left(c_\theta^2 - \frac{(c_\theta + 1)^2}{1 - c_\theta} + 1\right)\right]\,, \tag{4.18}$$

where c_θ is the outgoing electron angle and $c_{\rm min}, c_{\rm max}$ are either the acceptance or 0 for the forward/backward case. Estimating the theoretical uncertainties on this expression is delicate, although it is clear that the theoretical prediction for $\Gamma_{\phi ee}$ plays the leading role. We can get an estimate of this effect by using the lattice result f_ϕ. The most recent estimate [84] gives $f_\phi = 241 \pm 9 \pm 2\,\text{MeV}$. However, an earlier lattice estimate [91] found $f_\phi = 308 \pm 29\,\text{MeV}$ which, in spite of the much larger error, differs from the result of ref. [84] by more than 2σ. Another earlier estimate [92] found a central value in agreement with ref. [84] but with twice the error $f_\phi = 241 \pm 18\,\text{MeV}$. This latter uncertainty would correspond to a $1.8 \cdot 10^{-3}$ uncertainty on $\Delta A_{\rm FB}$, while the difference between the central values of refs. [84] and [91] would translate into an uncertainty of $\approx 6.7 \cdot 10^{-3}$.

[14] See e.g. ref. [87] for more details on the Vector Meson Dominance approach (VMD) which has been widely used in recent dark sector literature [88–90] for the ϕ and dark photon-related amplitudes.

JHEP06(2022)122

From our simulations, we obtain a theoretical prediction for the contribution from Bhabha and the ϕ resonance of $\Delta A_{\rm FB}^{\rm th} = 12.0 \cdot 10^{-3}$ which also differs from the experimental measurement by $2.8 \cdot 10^{-3}$. Altogether, it is clear that additional theoretical input on the ϕ interference contribution would be required to match the experimental precision. We will therefore present in the rest of this work both a conservative estimate based on the discrepancy between the lattice estimate of refs. [84] and [91] (corresponding to a $\sim {}^{+7.0}_{-5.5} \cdot 10^{-3}$ error), and a more aggressive limit based only on the difference between our estimate of the SM ϕ contribution and the measurement ($\sim \pm 3 \cdot 10^{-3}$). If we neglect the interference term and consider the small width regime $\Gamma_V < \Gamma_\phi$, then for the case of maximum negative shift, $m_V \simeq \sqrt{s_-}$, we have $\Delta A_{\rm FB}^{\rm NP} \simeq -\delta_R(\sqrt{s_-})/2$. For the "aggressive" limit this translates into a maximum shift on the luminosity of $\delta_R \simeq 1.2\%$. As shown in figure 2, this still allows to bring KLOE in agreement within 2σ with BaBar.

In practice, the interference contribution is also important and allows for somewhat larger shifts due to cancellations between both terms, as is confirmed by the full numerical results. Furthermore, the above limit is strongly reduced for larger width with a Γ_ϕ^2/Γ_V^2 suppression of $\Delta A_{\rm FB}^{\rm NP}$ when $\Gamma_\phi \ll \Gamma_V$. Finally, while the analysis in ref. [43] relied on a very precise calibration of the CoM energy, this was not the case for the study used to derive the $a_\mu^{\rm HVP}$ KLOE contribution. As can be seen e.g. from figure 7 of ref. [71], the spread in the CoM energy is larger, of the order of MeV, and this is related to the method used to measure the hadronic cross-section via ISR. Since we are primarily interested in this measurement, then we need to consider an uncertainty on m_V of the same order.[15]

Although limited by theoretical uncertainty, the forward-backward asymmetry measurement can provide significant constraints on our scenario. This mostly occurs because in the particular iDM model we have considered, the V width (see eq. (3.11)) is always in the MeV range. It would certainly be interesting to have a more complete experimental dataset, leveraging this observable to constrain this type of physics, for example from the CMD-3 experiment [34].

Finally, we did not include possible limits from the value of the ϕ partial width into muons reported in the same reference [43]. This is because firstly $\Gamma_{\phi\mu\mu}$ was inferred from cross-sections measurements only and thus has significantly larger experimental uncertainties, and moreover it is also sensitive to the Bhabha luminosity shift that we have described above. Secondly, it depends on the V coupling to muons, which do not directly enter our mechanism to shift $a_\mu^{\rm HVP}$, and also on the mass m_{χ_1} of the lightest dark matter particle, since for the $\mu^+\mu^-$ channel the experimental cuts on the missing energy are significantly tighter. Similar considerations can be applied to the estimates of $\Gamma_{\phi ee}$ derived from fitting measurements of cross-sections into hadronic final states.

4.6 Indirect effects on LEP precision measurements

A new vector boson of $\sim 1\,\text{GeV}$ mass can give rise to different types of indirect effects on LEP electroweak precision measurements. A first effect is a modification of the value of the

[15] This prevents us to use the asymmetries corresponding to the $\sqrt{s_0} \simeq m_\phi$ bin, since the two points are separated by an energy interval of the order of the uncertainty on m_V.

JHEP06(2022)122

electromagnetic coupling constant extrapolated at the large CoM energy scale of the LEP e^+e^- collisions, that can be written as

$$\alpha(s) = \frac{\alpha}{1 - \Delta\alpha_\ell(s) - \Delta\alpha_{\rm top}(s) - \Delta\alpha^{(5)}_{\rm had}(s)}\,, \tag{4.19}$$

where $\Delta\alpha_\ell$ and $\Delta\alpha_{\rm top}$ are the contribution to the photon vacuum polarization from the leptons and the top quark, which can be computed perturbatively with good accuracy, while the five-flavor hadronic contribution $\Delta\alpha^{(5)}_{\rm had}$ has to be extracted from data, and is determined by the dispersion relation

$$\Delta\alpha^{(5)}_{\rm had}(s) = \frac{s}{4\pi^2\alpha} P\!\int ds' \frac{\sigma_{\rm had}(s')}{s - s'}\,, \tag{4.20}$$

where P denotes the integral principal value. The important difference with the otherwise similar expression in eq. (2.1) is the $1/s$ factor in that equation which implies that low energy data play a dominant role for a_μ, while e.g. for $s \simeq M_Z^2$ the low energy contribution to the integral in eq. (4.20) is much less relevant. Hence, an increased value of the KLOE result for $\sigma_{\rm had}$ in the [0.6,0.9] GeV energy range is unlikely to affect the overall agreement with the LEP electroweak precision data (see also the dedicated analyses in refs. [93, 94]).

Additional subtle effects are related to corrections to luminosity measurements. The importance of a reliable determination of the LEP luminosity is well exemplified by the recent reassessment of the LEP measurement of the number of light active neutrino species N_ν [95]. During the first phase (LEP-1) high statistics data were collected at and around the Z pole, providing a wealth of measurements with sub-percent precision [96]. In particular, the value of N_ν was estimated from the measurement of the hadronic peak cross section $\sigma^{\rm peak}_{\rm had}$ by means of the relation

$$N_\nu \left(\frac{\Gamma^{\rm SM}_\nu}{\Gamma^{\rm SM}_\ell}\right) = \left(\frac{12\pi}{m_Z^2}\frac{R^0_\ell}{\sigma^{\rm peak}_{\rm had}}\right) - R^0_\ell - 3 - \delta_\tau \tag{4.21}$$

where $\Gamma^{\rm SM}_{\nu,\ell}$ are the SM predictions for the partial Z decay width into neutrinos and (massless) charged leptons, R^0_ℓ is the ratio between the Z branching fractions into hadrons and leptons and $\delta_\tau \sim 2.26 \times 10^{-3}$ accounts for a small correction from finite m_τ effects on the $\Gamma^{\rm SM}_\tau$ partial width. The combination of the measurements made by the four LEP experiments [96] led to: $N_\nu = 2.9840 \pm 0.0082$ which had a 2σ tension with the canonical SM value $N^{\rm SM}_\nu = 3$. The measurement is directly affected by biased errors in estimating the integrated luminosity only through $\sigma^{\rm peak}_{\rm had}$, all other quantities in eq. (4.21) instead do not depend on the absolute luminosity. Indeed, the uncertainty on the integrated luminosity represents the largest contribution to the uncertainty on N_ν. The LEP luminosity was determined by comparing the measured rate of Bhabha-scattering process at small angles with the SM prediction. Recently this determination has been reassessed first by correcting for a bias in the luminosity measurement due to the large charge density of the particle bunches which modify (decrease) the effective acceptance of the luminometer [95], and next by using an updated and more accurate prediction of the Bhabha cross section which is found to reduce its value by about 0.048% [97]. Both effects go in the direction of decreasing

JHEP06(2022)122

the Bhabha cross section with respect to that used in the LEP fit [96], thus increasing the effective luminosity, decreasing $\sigma^0_{\rm had}$, and eventually raising the inferred value of active neutrino species to $N_\nu = 2.9963 \pm 0.0074$, in perfect agreement with the SM.

The direct effect of a (constructive) NP contribution to the Bhabha cross section would instead go in the opposite direction, decreasing the estimated luminosity, and hence increasing $\sigma^{\rm peak}_{\rm had}$ and reducing N_ν. However, at LEP energies the $m_V \sim 1\,\text{GeV}$ vector boson grossly behaves like a massive photon with ε-suppressed couplings to electrons/positrons. The most relevant effect will then come from t-channel γ-V interference, which in our case is suppressed by a relative $\varepsilon^2 \sim 10^{-4}$, and thus negligible. An additional indirect effect is again related to adjustments in the value of the hadronic vacuum polarization that enters the t-channel photon propagator, and that could modify the value of the $\alpha(t)$ input to the LEP Bhabha event generators [53]. Yet, given that at the small Bhabha scattering angles/small momentum transfer ($\theta \lesssim 60\,\text{mrad}$, $t \lesssim (2.8\,\text{GeV})^2$) specific of the LEP luminosity measurements the hadronic contribution remains small ($\Delta\alpha^{(5)}_{\rm had} \lesssim 0.008$ and at most $\sim 30\%$ of the total vacuum polarization, see e.g. ref. [53]) the corresponding correction remains below the systematic uncertainties. It is interesting to note that, although both the direct contribution of V to Bhabha scattering and the indirect effect of increasing the value of $\Delta\alpha^{(5)}_{\rm had}$ affect negligibly the LEP luminosity measurement, they go in the same direction and, for example, both would tend to decrease the central value of N_ν.

4.7 LEP limit on $V - Z$ mixing

In the inelastic dark matter model, the interaction between the dark photon and the SM particles proceed via kinetic mixing between the $\text{U}(1)_V$ and the $\text{U}(1)_Y$ field strength. This implies that after electroweak symmetry breaking, the Z boson mixes with the dark photon, leading to a small modification of the SM electroweak couplings. A complete fit for this effect in the electroweak precision observables was performed in [98, 99] leading to the relatively model independent bound:

$$\varepsilon < 0.027 \quad \text{(LEP - EW fit)}\,. \tag{4.22}$$

5 Joint solution to the a_μ-related anomalies

In this section we study in which range of parameters for the model outlined in section 3.1 the indirect NP-induced effects on a_μ, discussed in the sections 2.2 and 2.3, together with the direct loop contributions of the new vector boson V can optimally resolve the various a_μ related discrepancies.

First we present in figure 5 the parameter space in which one can obtain a simultaneous fit to both the BaBar/KLOE discrepancy and the a_μ at the 2σ-level. The blue region denotes the values of ε where the KLOE result is within 2σ of the BaBar measurement assuming that the BaBar result is not modified, while the green region is the area where a_μ fits the experimental result at the 2σ-level (with both the shift in the data-driven estimate and the new physics contribution included). As expected from the resonant nature of the production mechanism, the shift in KLOE data brings it in agreement with BaBar only in

JHEP06(2022)122

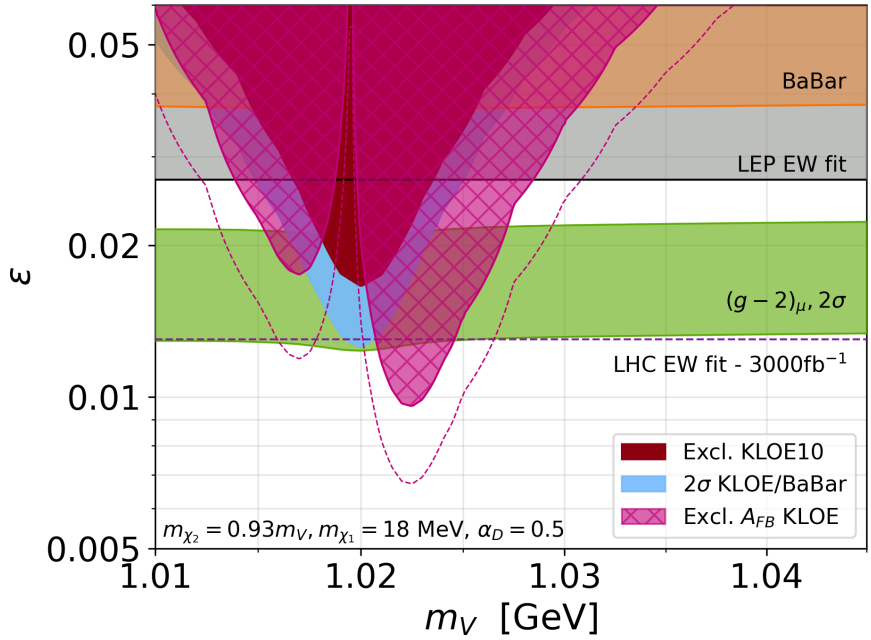

Figure 5. Parameter range compatible at 2σ with the experimental measurement of Δa_μ (green region) resulting from a redetermination of the KLOE luminosity, for $\alpha_D = 0.5, m_{\chi_2} = 0.93\ m_V$ and $m_{\chi_1} = 18\,\text{MeV}$. In the blue region the KLOE and BaBar results for σ_{had} are brought into agreement at 2σ. The red region corresponds to a shift of the KLOE measurement in tension with BaBar (and with the other experiments) at more than 2σ. The limit from the electroweak fit at LEP (gray band), the projection for LHC run-3 [99] (violet dashed line), and the recasting of the BaBar limit [74] (orange band) are also shown (see text). The hatched magenta region corresponds to the conservative 2σ exclusion from ΔA_{FB}, while the magenta dashed line corresponds to the more aggressive exclusion limit (see text).

a narrow region around the ϕ mass. Depending on the strength of the shift, it can account for up to one-quarter of the full anomaly before leading to new tensions with the rest of the data-driven experimental results. Conversely, our results can be interpreted as a new exclusion limit for this type of dark photons centred around the GeV (represented as the red area in the figure) for which the shift lead to 3σ internal tension between the different KLOE measurements. We note that similar exclusions likely exist around the CoM energy of the different experiments using Bhabha scattering to calibrate their luminosity. The magenta area represents the 2σ "conservative" exclusion using the ΔA_{FB} measurement as presented in section 4.5, while the dashed magenta line is the "aggressive" exclusion.

When the dark photon mass becomes close to 1 GeV, the KLOE10 [42] analysis result will receive a correction similar to the one for KLOE08 at $m_V \sim 1.02\,\text{GeV}$. While this circumvents efficiently all the ϕ-meson related constraints, it also provides a significantly weaker overall effect since both the KLOE08 and KLOE12 result are not modified. It can nonetheless provide a definite improvement in the overall agreement between the data-driven method and the lattice BMW result, although with a NP contribution almost overshooting the a_μ anomaly. Finally, the shift in BESIII does not rely on a tuned m_V value and will be active for all vector masses in the GeV region. If a similar effect could be quantitatively

JHEP06(2022)122

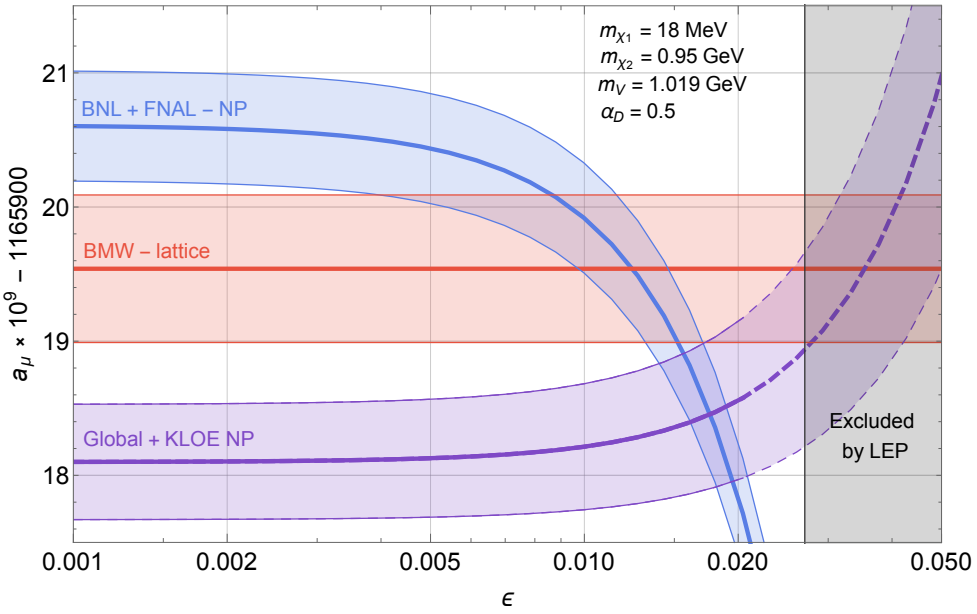

Figure 6. Theoretical prediction (purple) for a_μ as a function of ε for a dark photon model with $m_{\chi_1} = 18\,\text{MeV}$, $m_{\chi_2} = 0.9\,\text{GeV}$, $m_V = 1.019\,\text{GeV}$ and $\alpha_D = 0.5$. The dashed purple curve denotes the region where the KLOE08 and KLOE10 results are more than 3σ away. The blue band corresponds to the combined BNL and FNAL experimental results after subtracting the direct NP contribution from the dark photon. The red band shows the prediction obtained with the BMW lattice estimate of $a_\mu^{\text{LO,HVP}}$. The width of the bands represents $1\,\sigma$ uncertainties. The grey region is excluded by LEP.

shown to exist in BaBar, it would represent a generic mechanism to reduce the discrepancies with the BMW lattice estimate, although at the cost of increasing the tension with the KLOE results.

In figure 6 we show in purple the $\pm 1\sigma$ band for the theoretical prediction of a_μ as a function of ε for $m_{\chi_1} = 18\,\text{MeV}$, $m_{\chi_2} = 0.95\,\text{GeV}$, $m_V = 1.019\,\text{GeV}$ and $\alpha_D = 0.5$. Since our analysis only includes the correction to a_μ^{HVP} in the $\sqrt{s} \in [0.6, 0.9]\,\text{GeV}$ range, we use a theoretical uncertainty on our result of 35% to account for the missing contribution. The dashed curve denotes the values of ε for which the KLOE08 result is more than 3σ away from the KLOE10 measurement. The red region shows the $\pm 1\sigma$ BMW-lattice computation and the blue region shows the $\pm 1\sigma$ band for the BNL and FNAL experimental results after subtracting the direct contribution to a_μ. The grey area is excluded by a fit to the electroweak SM couplings at LEP, see eq. (4.22). Therefore, this figure shows the interplay between the indirect effect of correcting the KLOE08, KLOE12 and BESIII results (purple curve) and the direct NP contribution to a_μ (blue curve), and identifies the regions where the experimental result and the lattice and data-driven computation become compatible at the $\sim 2\sigma$ level. In particular the figure shows that with a specific choice of the model parameters it is possible to bring the data-driven theoretical prediction in good agreement with the experimental result while reducing the discrepancy with the prediction based on the lattice computation below the $\sim 2\sigma$ level.

JHEP06(2022)122

6 Conclusions

In this work, we have explored the intriguing possibility that a feebly interacting particle with mass around the ϕ resonance, that would be produced in e^+e^- collisions whenever $\sqrt{s} \geq m_\phi$, could contribute to the measured number of e^+e^- and $\mu^+\mu^-$ events. This could affect significantly the estimated luminosity from Bhabha events, thus affecting the determination of $\sigma_{\rm had}$ from the number of hadronic final state. It would furthermore contribute to the ratio between ISR $\pi\pi\gamma$ and $\mu\mu\gamma$ events used in luminosity independent measurements of $\sigma_{\rm had}$, implying that some corrections must be applied before the experimental results could be related to the hadronic contribution to the photon vacuum polarization. Finally it would also require a reinterpretation of the results on measurements of the di-muon cross-section. Such a cascade of rather subtle indirect effects can result in increasing the data-driven estimate of $a_\mu^{\rm HVP}$ by a few percent, which suffices to solve the tension between the KLOE and BaBar determinations of $\sigma_{\rm had}$, and to reconcile the estimate of the hadronic vacuum polarisation contribution $a_\mu^{\rm HVP}$ from the data-driven dispersive method with the latest lattice calculation [31] (as well as with the estimate of $a_\mu^{\rm HVP}$ from τ hadronic decays).

To illustrate the viability of this mechanism, we have constructed an explicit model based on a iDM paradigm which includes a vector particle mediator V with mass $m_V \sim 1\,\text{GeV}$. V decays mainly proceed via a semi-visible leptonic channel, and can mimic effectively the Bhabha signature altering the estimated value of the luminosity at KLOE08, and produce the required excess of semi-visible muonic final states in the KLOE12 and BESIII analyses. We have found that in our model the indirect effects by themselves are not sufficient to solve completely the discrepancy between the experimental determination of a_μ and the prediction. However, the vector boson mediator will also contribute directly to a_μ via genuine NP loop contributions, and we find that when direct and indirect effects are considered together, the a_μ discrepancy can indeed be solved, (with about 1/4 of the discrepancy accounted by indirect effects, and 3/4 by direct loop effects). Clearly, the new vector boson will also contribute to the anomalous magnetic moment of the electron $(g-2)_e$. However, the corresponding correction is strongly suppressed by the naive rescaling factor m_e^2/m_μ^2, which ensures that the NP effect remains an order of magnitude below the current constraints. The simple model that we have put forth also provides an adequate light dark matter candidate with a rich phenomenology which might be worthwhile exploring further. On the long run, we hope that our work can provide further motivations to the search for similar "stealthy" dark photons characterised by the required semi-visible decays. Eventually, since the most important effect in our construction is that of shifting $a_\mu^{\rm HVP}$ to larger values, a crucial test of the whole idea could come from the MuonE experiment [100–103], as well as from new high precision determinations of $a_\mu^{\rm HVP}$ on the lattice.

Note added. As this paper was being finalised, the work [104] appeared which studied the possibility of reconciling the data driven and the lattice determinations of $a_\mu^{\rm HVP}$ by invoking a light NP mediator that directly modifies $\sigma_{\rm had}$. The authors concluded that such a possibility is excluded by a number of experimental constraints. The NP effect explored in this work is of a completely different nature, and it leads to different conclusions. In first

JHEP06(2022)122

place, it does not modify directly $\sigma_{\rm had}$ at a significant level. Moreover, as we have shown, besides allowing to reconcile the data driven and the lattice determination of $a_\mu^{\rm HVP}$, it can also bring into agreement the KLOE and BaBar results for $\sigma_{\rm had}$.

Acknowledgments

We are indebted with G. Venanzoni for pointing out to us the KLOE12 luminosity independent determination of $\sigma_{\rm had}$ [36] that triggered the revision of a first draft, and with S. Müller for valuable information on the KLOE12 analysis. We thank M. Raggi and T. Spadaro for discussions, and F. Piccinini and C.M. Carloni Calame for providing us with details on the BabaYaga event generator. LD thanks Olcyr Sumensari and Diego Guadagnoli for useful discussions. This work has received support by the INFN Iniziativa Specifica Theoretical Astroparticle Physics (TAsP). G.G.d.C. is supported by the Frascati National Laboratories (LNF) through a Cabibbo Fellowship, call 2019. This project has received funding from the European Union's Horizon 2020 research and innovation programme under the Marie Sklodowska-Curie grant agreement No. 101028626.

References

[1] Muon $g-2$ collaboration, *Measurement of the Positive Muon Anomalous Magnetic Moment to 0.46 ppm*, *Phys. Rev. Lett.* **126** (2021) 141801 [arXiv:2104.03281] [INSPIRE].

[2] Muon $g-2$ collaboration, *Final Report of the Muon E821 Anomalous Magnetic Moment Measurement at BNL*, *Phys. Rev. D* **73** (2006) 072003 [hep-ex/0602035] [INSPIRE].

[3] T. Aoyama et al., *The anomalous magnetic moment of the muon in the Standard Model*, *Phys. Rept.* **887** (2020) 1 [arXiv:2006.04822] [INSPIRE].

[4] T. Aoyama, M. Hayakawa, T. Kinoshita and M. Nio, *Complete Tenth-Order QED Contribution to the Muon $g-2$*, *Phys. Rev. Lett.* **109** (2012) 111808 [arXiv:1205.5370] [INSPIRE].

[5] T. Aoyama, T. Kinoshita and M. Nio, *Theory of the Anomalous Magnetic Moment of the Electron*, *Atoms* **7** (2019) 28 [INSPIRE].

[6] A. Czarnecki, W.J. Marciano and A. Vainshtein, *Refinements in electroweak contributions to the muon anomalous magnetic moment*, *Phys. Rev. D* **67** (2003) 073006 [*Erratum ibid.* **73** (2006) 119901] [hep-ph/0212229] [INSPIRE].

[7] C. Gnendiger, D. Stöckinger and H. Stöckinger-Kim, *The electroweak contributions to $(g-2)_\mu$ after the Higgs boson mass measurement*, *Phys. Rev. D* **88** (2013) 053005 [arXiv:1306.5546] [INSPIRE].

[8] M. Davier, A. Hoecker, B. Malaescu and Z. Zhang, *Reevaluation of the hadronic vacuum polarisation contributions to the Standard Model predictions of the muon $g-2$ and $\alpha(m_Z^2)$ using newest hadronic cross-section data*, *Eur. Phys. J. C* **77** (2017) 827 [arXiv:1706.09436] [INSPIRE].

JHEP06(2022)122

[9] A. Keshavarzi, D. Nomura and T. Teubner, *Muon $g-2$ and $\alpha(M_Z^2)$: a new data-based analysis*, *Phys. Rev. D* **97** (2018) 114025 [arXiv:1802.02995] [INSPIRE].

[10] G. Colangelo, M. Hoferichter and P. Stoffer, *Two-pion contribution to hadronic vacuum polarization*, *JHEP* **02** (2019) 006 [arXiv:1810.00007] [INSPIRE].

[11] M. Hoferichter, B.-L. Hoid and B. Kubis, *Three-pion contribution to hadronic vacuum polarization*, *JHEP* **08** (2019) 137 [arXiv:1907.01556] [INSPIRE].

[12] M. Davier, A. Hoecker, B. Malaescu and Z. Zhang, *A new evaluation of the hadronic vacuum polarisation contributions to the muon anomalous magnetic moment and to $\alpha(m_Z^2)$*, *Eur. Phys. J. C* **80** (2020) 241 [*Erratum ibid.* **80** (2020) 410] [arXiv:1908.00921] [INSPIRE].

[13] A. Keshavarzi, D. Nomura and T. Teubner, *$g-2$ of charged leptons, $\alpha(M_Z^2)$, and the hyperfine splitting of muonium*, *Phys. Rev. D* **101** (2020) 014029 [arXiv:1911.00367] [INSPIRE].

[14] A. Kurz, T. Liu, P. Marquard and M. Steinhauser, *Hadronic contribution to the muon anomalous magnetic moment to next-to-next-to-leading order*, *Phys. Lett. B* **734** (2014) 144 [arXiv:1403.6400] [INSPIRE].

[15] K. Melnikov and A. Vainshtein, *Hadronic light-by-light scattering contribution to the muon anomalous magnetic moment revisited*, *Phys. Rev. D* **70** (2004) 113006 [hep-ph/0312226] [INSPIRE].

[16] P. Masjuan and P. Sanchez-Puertas, *Pseudoscalar-pole contribution to the $(g_\mu-2)$: a rational approach*, *Phys. Rev. D* **95** (2017) 054026 [arXiv:1701.05829] [INSPIRE].

[17] G. Colangelo, M. Hoferichter, M. Procura and P. Stoffer, *Dispersion relation for hadronic light-by-light scattering: two-pion contributions*, *JHEP* **04** (2017) 161 [arXiv:1702.07347] [INSPIRE].

[18] M. Hoferichter, B.-L. Hoid, B. Kubis, S. Leupold and S.P. Schneider, *Dispersion relation for hadronic light-by-light scattering: pion pole*, *JHEP* **10** (2018) 141 [arXiv:1808.04823] [INSPIRE].

[19] A. Gérardin, H.B. Meyer and A. Nyffeler, *Lattice calculation of the pion transition form factor with $N_f = 2+1$ Wilson quarks*, *Phys. Rev. D* **100** (2019) 034520 [arXiv:1903.09471] [INSPIRE].

[20] J. Bijnens, N. Hermansson-Truedsson and A. Rodríguez-Sánchez, *Short-distance constraints for the HLbL contribution to the muon anomalous magnetic moment*, *Phys. Lett. B* **798** (2019) 134994 [arXiv:1908.03331] [INSPIRE].

[21] G. Colangelo, F. Hagelstein, M. Hoferichter, L. Laub and P. Stoffer, *Longitudinal short-distance constraints for the hadronic light-by-light contribution to $(g-2)_\mu$ with large-N_c Regge models*, *JHEP* **03** (2020) 101 [arXiv:1910.13432] [INSPIRE].

[22] T. Blum et al., *Hadronic Light-by-Light Scattering Contribution to the Muon Anomalous Magnetic Moment from Lattice QCD*, *Phys. Rev. Lett.* **124** (2020) 132002 [arXiv:1911.08123] [INSPIRE].

[23] G. Colangelo, M. Hoferichter, A. Nyffeler, M. Passera and P. Stoffer, *Remarks on higher-order hadronic corrections to the muon $g-2$*, *Phys. Lett. B* **735** (2014) 90 [arXiv:1403.7512] [INSPIRE].

[24] KLOE-2 collaboration, *Combination of KLOE $\sigma\left(e^+e^- \to \pi^+\pi^-\gamma(\gamma)\right)$ measurements and determination of $a_\mu^{\pi^+\pi^-}$ in the energy range $0.10 < s < 0.95\ GeV^2$*, *JHEP* **03** (2018) 173 [arXiv:1711.03085] [INSPIRE].

JHEP06(2022)122

[25] BaBar collaboration, *Precise measurement of the $e^+e^- \to \pi^+\pi^-$ (gamma) cross section with the Initial State Radiation method at BABAR*, *Phys. Rev. Lett.* **103** (2009) 231801 [arXiv:0908.3589] [INSPIRE].

[26] CMD-2 collaboration, *Reanalysis of hadronic cross-section measurements at CMD-2*, *Phys. Lett. B* **578** (2004) 285 [hep-ex/0308008] [INSPIRE].

[27] V.M. Aul'chenko et al., *Measurement of the $e^+e^- \to \pi^+\pi^-$ cross section with the CMD-2 detector in the* 370–520*-MeV energy range*, *JETP Lett.* **84** (2006) 413 [hep-ex/0610016] [INSPIRE].

[28] CMD-2 collaboration, *High-statistics measurement of the pion form factor in the rho-meson energy range with the CMD-2 detector*, *Phys. Lett. B* **648** (2007) 28 [hep-ex/0610021] [INSPIRE].

[29] M.N. Achasov et al., *Update of the $e^+e^- \to \pi^+\pi^-$ cross-section measured by SND detector in the energy region $400 < s^{1/2} < 1000$ MeV*, *J. Exp. Theor. Phys.* **103** (2006) 380 [hep-ex/0605013] [INSPIRE].

[30] BESIII collaboration, *Measurement of the $e^+e^- \to \pi^+\pi^-$ cross section between* 600 *and* 900 *MeV using initial state radiation*, *Phys. Lett. B* **753** (2016) 629 [*Erratum ibid.* **812** (2021) 135982] [arXiv:1507.08188] [INSPIRE].

[31] S. Borsányi et al., *Leading hadronic contribution to the muon magnetic moment from lattice QCD*, *Nature* **593** (2021) 51 [arXiv:2002.12347] [INSPIRE].

[32] A. Keshavarzi, K.S. Khaw and T. Yoshioka, *Muon $g-2$: A review*, *Nucl. Phys. B* **975** (2022) 115675 [arXiv:2106.06723] [INSPIRE].

[33] A. Gérardin, *The anomalous magnetic moment of the muon: status of Lattice QCD calculations*, *Eur. Phys. J. A* **57** (2021) 116 [arXiv:2012.03931] [INSPIRE].

[34] A.E. Ryzhenenkov et al., *Overview of the CMD-3 recent results*, *J. Phys. Conf. Ser.* **1526** (2020) 012009 [INSPIRE].

[35] KLOE collaboration, *Measurement of $\sigma(e^+e^- \to \pi^+\pi^-\gamma(\gamma)$ and the dipion contribution to the muon anomaly with the KLOE detector*, *Phys. Lett. B* **670** (2009) 285 [arXiv:0809.3950] [INSPIRE].

[36] KLOE collaboration, *Precision measurement of $\sigma(e^+e^- \to \pi^+\pi^-\gamma)/\sigma(e^+e^- \to \mu^+\mu^-\gamma)$ and determination of the $\pi^+\pi^-$ contribution to the muon anomaly with the KLOE detector*, *Phys. Lett. B* **720** (2013) 336 [arXiv:1212.4524] [INSPIRE].

[37] BaBar collaboration, *Precise Measurement of the $e^+e^- \to \pi^+\pi^-(\gamma)$ Cross Section with the Initial-State Radiation Method at BABAR*, *Phys. Rev. D* **86** (2012) 032013 [arXiv:1205.2228] [INSPIRE].

[38] E. Izaguirre, G. Krnjaic and B. Shuve, *Discovering Inelastic Thermal-Relic Dark Matter at Colliders*, *Phys. Rev. D* **93** (2016) 063523 [arXiv:1508.03050] [INSPIRE].

[39] E. Izaguirre, Y. Kahn, G. Krnjaic and M. Moschella, *Testing Light Dark Matter Coannihilation With Fixed-Target Experiments*, *Phys. Rev. D* **96** (2017) 055007 [arXiv:1703.06881] [INSPIRE].

[40] J.R. Jordan, Y. Kahn, G. Krnjaic, M. Moschella and J. Spitz, *Signatures of Pseudo-Dirac Dark Matter at High-Intensity Neutrino Experiments*, *Phys. Rev. D* **98** (2018) 075020 [arXiv:1806.05185] [INSPIRE].

JHEP06(2022)122

[41] A. Berlin and F. Kling, *Inelastic Dark Matter at the LHC Lifetime Frontier: ATLAS, CMS, LHCb, CODEX-b, FASER, and MATHUSLA*, *Phys. Rev. D* **99** (2019) 015021 [arXiv:1810.01879] [INSPIRE].

[42] KLOE collaboration, *Measurement of $\sigma(e^+e^- \to \pi^+\pi^-)$ from threshold to 0.85 GeV^2 using Initial State Radiation with the KLOE detector*, *Phys. Lett. B* **700** (2011) 102 [arXiv:1006.5313] [INSPIRE].

[43] KLOE collaboration, *Measurement of the leptonic decay widths of the phi-meson with the KLOE detector*, *Phys. Lett. B* **608** (2005) 199 [hep-ex/0411082] [INSPIRE].

[44] S.J. Brodsky and E. De Rafael, *Suggested boson-lepton pair couplings and the anomalous magnetic moment of the muon*, *Phys. Rev.* **168** (1968) 1620 [INSPIRE].

[45] B.E. Lautrup and E. De Rafael, *Calculation of the sixth-order contribution from the fourth-order vacuum polarization to the difference of the anomalous magnetic moments of muon and electron*, *Phys. Rev.* **174** (1968) 1835 [INSPIRE].

[46] F. Jegerlehner, *The Anomalous Magnetic Moment of the Muon*, vol. 274, Springer, Cham, Germany (2017) [DOI] [INSPIRE].

[47] M. Benayoun, L. Delbuono and F. Jegerlehner, *$BHLS_2$, a New Breaking of the HLS Model and its Phenomenology*, *Eur. Phys. J. C* **80** (2020) 81 [*Erratum ibid.* **80** (2020) 244] [arXiv:1903.11034] [INSPIRE].

[48] B. Ananthanarayan, I. Caprini and D. Das, *Pion electromagnetic form factor at high precision with implications to $a_\mu^{\pi\pi}$ and the onset of perturbative QCD*, *Phys. Rev. D* **98** (2018) 114015 [arXiv:1810.09265] [INSPIRE].

[49] M. Davier, A. Hoecker, B. Malaescu and Z. Zhang, *Reevaluation of the Hadronic Contributions to the Muon $g-2$ and to $\alpha(M_Z^2)$*, *Eur. Phys. J. C* **71** (2011) 1515 [*Erratum ibid.* **72** (2012) 1874] [arXiv:1010.4180] [INSPIRE].

[50] M. Davier et al., *The Discrepancy Between tau and e^+e^- Spectral Functions Revisited and the Consequences for the Muon Magnetic Anomaly*, *Eur. Phys. J. C* **66** (2010) 127 [arXiv:0906.5443] [INSPIRE].

[51] M. Davier, A. Höcker, B. Malaescu, C.-Z. Yuan and Z. Zhang, *Update of the ALEPH non-strange spectral functions from hadronic τ decays*, *Eur. Phys. J. C* **74** (2014) 2803 [arXiv:1312.1501] [INSPIRE].

[52] M. Bruno, T. Izubuchi, C. Lehner and A. Meyer, *On isospin breaking in τ decays for $(g-2)_\mu$ from Lattice QCD*, *PoS* **LATTICE2018** (2018) 135 [arXiv:1811.00508] [INSPIRE].

[53] S. Jadach et al., *Event generators for Bhabha scattering*, in *CERN Workshop on LEP2 Physics (followed by 2nd meeting, 15–16 Jun 1995 and 3rd meeting 2–3 Nov 1995)*, (1996) [DOI] [hep-ph/9602393] [INSPIRE].

[54] A.B. Arbuzov, G.V. Fedotovich, F.V. Ignatov, E.A. Kuraev and A.L. Sibidanov, *Monte-Carlo generator for e^+e^- annihilation into lepton and hadron pairs with precise radiative corrections*, *Eur. Phys. J. C* **46** (2006) 689 [hep-ph/0504233] [INSPIRE].

[55] G. Balossini, C.M. Carloni Calame, G. Montagna, O. Nicrosini and F. Piccinini, *Matrix elements and Parton Shower in the event generator BABAYAGA*, *Nucl. Phys. B Proc. Suppl.* **162** (2006) 59 [hep-ph/0610022] [INSPIRE].

[56] B. Holdom, *Two* U(1)*'s and Epsilon Charge Shifts*, *Phys. Lett. B* **166** (1986) 196 [INSPIRE].

JHEP06(2022)122

[57] P. Fayet, *The light U boson as the mediator of a new force, coupled to a combination of Q, B, L and dark matter*, *Eur. Phys. J. C* **77** (2017) 53 [arXiv:1611.05357] [INSPIRE].

[58] B. Batell, J. Berger, L. Darmé and C. Frugiuele, *Inelastic dark matter at the Fermilab Short Baseline Neutrino Program*, *Phys. Rev. D* **104** (2021) 075026 [arXiv:2106.04584] [INSPIRE].

[59] L. Darmé, S. Rao and L. Roszkowski, *Light dark Higgs boson in minimal sub-GeV dark matter scenarios*, *JHEP* **03** (2018) 084 [arXiv:1710.08430] [INSPIRE].

[60] L. Darmé, S. Rao and L. Roszkowski, *Signatures of dark Higgs boson in light fermionic dark matter scenarios*, *JHEP* **12** (2018) 014 [arXiv:1807.10314] [INSPIRE].

[61] G.N. Wojcik and T.G. Rizzo, *Forbidden scalar dark matter and dark Higgses*, *JHEP* **04** (2022) 033 [arXiv:2109.07369] [INSPIRE].

[62] P. Asadi, T.R. Slatyer and J. Smirnov, *WIMPs Without Weakness: Generalized Mass Window with Entropy Injection*, arXiv:2111.11444 [INSPIRE].

[63] A. Fradette and M. Pospelov, *BBN for the LHC: constraints on lifetimes of the Higgs portal scalars*, *Phys. Rev. D* **96** (2017) 075033 [arXiv:1706.01920] [INSPIRE].

[64] M. Kawasaki, K. Kohri, T. Moroi and Y. Takaesu, *Revisiting Big-Bang Nucleosynthesis Constraints on Long-Lived Decaying Particles*, *Phys. Rev. D* **97** (2018) 023502 [arXiv:1709.01211] [INSPIRE].

[65] N.D. Christensen et al., *A Comprehensive approach to new physics simulations*, *Eur. Phys. J. C* **71** (2011) 1541 [arXiv:0906.2474] [INSPIRE].

[66] C. Degrande, C. Duhr, B. Fuks, D. Grellscheid, O. Mattelaer and T. Reiter, *UFO — The Universal FeynRules Output*, *Comput. Phys. Commun.* **183** (2012) 1201 [arXiv:1108.2040] [INSPIRE].

[67] A. Alloul, N.D. Christensen, C. Degrande, C. Duhr and B. Fuks, *FeynRules 2.0 — A complete toolbox for tree-level phenomenology*, *Comput. Phys. Commun.* **185** (2014) 2250 [arXiv:1310.1921] [INSPIRE].

[68] J. Alwall et al., *The automated computation of tree-level and next-to-leading order differential cross sections, and their matching to parton shower simulations*, *JHEP* **07** (2014) 079 [arXiv:1405.0301] [INSPIRE].

[69] CMD-2 collaboration, *Measurement of $e^+e^- \to \pi^+\pi^-$ cross-section with CMD-2 around ρ-meson*, *Phys. Lett. B* **527** (2002) 161 [hep-ex/0112031] [INSPIRE].

[70] M.N. Achasov et al., *Study of the process $e^+e^- \to \pi^+\pi^-$ in the energy region $400 < s^{1/2} < 1000$ MeV*, *J. Exp. Theor. Phys.* **101** (2005) 1053 [hep-ex/0506076] [INSPIRE].

[71] KLOE collaboration, *Measurement of the DAFNE luminosity with the KLOE detector using large angle Bhabha scattering*, *Eur. Phys. J. C* **47** (2006) 589 [hep-ex/0604048] [INSPIRE].

[72] BaBar collaboration, *Time-Integrated Luminosity Recorded by the BABAR Detector at the PEP-II e^+e^- Collider*, *Nucl. Instrum. Meth. A* **726** (2013) 203 [arXiv:1301.2703] [INSPIRE].

[73] BESIII collaboration, *Measurement of the integrated luminosities of the data taken by BESIII at $\sqrt{s} = 3.650$ and 3.773 GeV*, *Chin. Phys. C* **37** (2013) 123001 [arXiv:1307.2022] [INSPIRE].

[74] BaBar collaboration, *Search for a Dark Photon in e^+e^- Collisions at BaBar*, *Phys. Rev. Lett.* **113** (2014) 201801 [arXiv:1406.2980] [INSPIRE].

JHEP06(2022)122

[75] BaBar collaboration, *The BABAR Detector: Upgrades, Operation and Performance*, *Nucl. Instrum. Meth. A* **729** (2013) 615 [arXiv:1305.3560] [INSPIRE].

[76] J. Seeman et al., *Status report on PEP-II performance*, in *7th European Particle Accelerator Conference (EPAC 2000)*, Vienna, Austria, 26–30 June 2000, pp. 38–42 (2002) [INSPIRE].

[77] BaBar collaboration, *Search for Invisible Decays of a Dark Photon Produced in e^+e^- Collisions at BaBar*, *Phys. Rev. Lett.* **119** (2017) 131804 [arXiv:1702.03327] [INSPIRE].

[78] BaBar collaboration, *Search for Production of Invisible Final States in Single-Photon Decays of $\Upsilon(1S)$*, *Phys. Rev. Lett.* **107** (2011) 021804 [arXiv:1007.4646] [INSPIRE].

[79] G. Mohlabeng, *Revisiting the dark photon explanation of the muon anomalous magnetic moment*, *Phys. Rev. D* **99** (2019) 115001 [arXiv:1902.05075] [INSPIRE].

[80] M. Duerr, T. Ferber, C. Hearty, F. Kahlhoefer, K. Schmidt-Hoberg and P. Tunney, *Invisible and displaced dark matter signatures at Belle II*, *JHEP* **02** (2020) 039 [arXiv:1911.03176] [INSPIRE].

[81] M. Duerr, T. Ferber, C. Garcia-Cely, C. Hearty and K. Schmidt-Hoberg, *Long-lived Dark Higgs and Inelastic Dark Matter at Belle II*, *JHEP* **04** (2021) 146 [arXiv:2012.08595] [INSPIRE].

[82] Belle-II collaboration, *The Belle II Physics Book*, *PTEP* **2019** (2019) 123C01 [*Erratum ibid.* **2020** (2020) 029201] [arXiv:1808.10567] [INSPIRE].

[83] S. Dreyer et al., *Physics reach of a long-lived particle detector at Belle II*, arXiv:2105.12962 [INSPIRE].

[84] χQCD collaboration, *Charmed and ϕ meson decay constants from 2+1-flavor lattice QCD*, *Chin. Phys. C* **45** (2021) 023109 [arXiv:2008.05208] [INSPIRE].

[85] Particle Data Group collaboration, *Review of Particle Physics*, *PTEP* **2020** (2020) 083C01 [INSPIRE].

[86] KLOE-2 collaboration, *Measurement of the running of the fine structure constant below 1 GeV with the KLOE Detector*, *Phys. Lett. B* **767** (2017) 485 [arXiv:1609.06631] [INSPIRE].

[87] T. Fujiwara, T. Kugo, H. Terao, S. Uehara and K. Yamawaki, *Nonabelian Anomaly and Vector Mesons as Dynamical Gauge Bosons of Hidden Local Symmetries*, *Prog. Theor. Phys.* **73** (1985) 926 [INSPIRE].

[88] S. Tulin, *New weakly-coupled forces hidden in low-energy QCD*, *Phys. Rev. D* **89** (2014) 114008 [arXiv:1404.4370] [INSPIRE].

[89] P. Ilten, Y. Soreq, M. Williams and W. Xue, *Serendipity in dark photon searches*, *JHEP* **06** (2018) 004 [arXiv:1801.04847] [INSPIRE].

[90] L. Darmé, L. Di Luzio, M. Giannotti and E. Nardi, *Selective enhancement of the QCD axion couplings*, *Phys. Rev. D* **103** (2021) 015034 [arXiv:2010.15846] [INSPIRE].

[91] ETM collaboration, *Meson masses and decay constants from unquenched lattice QCD*, *Phys. Rev. D* **80** (2009) 054510 [arXiv:0906.4720] [INSPIRE].

[92] HPQCD collaboration, *V_{cs} from $D_s \to \phi\ell\nu$ semileptonic decay and full lattice QCD*, *Phys. Rev. D* **90** (2014) 074506 [arXiv:1311.6669] [INSPIRE].

[93] A. Keshavarzi, W.J. Marciano, M. Passera and A. Sirlin, *Muon $g-2$ and $\Delta\alpha$ connection*, *Phys. Rev. D* **102** (2020) 033002 [arXiv:2006.12666] [INSPIRE].

JHEP06(2022)122

[94] A. Crivellin, M. Hoferichter, C.A. Manzari and M. Montull, *Hadronic Vacuum Polarization: $(g-2)_\mu$ versus Global Electroweak Fits*, *Phys. Rev. Lett.* **125** (2020) 091801 [arXiv:2003.04886] [INSPIRE].

[95] G. Voutsinas, E. Perez, M. Dam and P. Janot, *Beam-beam effects on the luminosity measurement at LEP and the number of light neutrino species*, *Phys. Lett. B* **800** (2020) 135068 [arXiv:1908.01704] [INSPIRE].

[96] ALEPH, DELPHI, L3, OPAL and SLD collaborations, LEP Electroweak Working Group, SLD Electroweak Group, SLD Heavy Flavour Group, *Precision electroweak measurements on the Z resonance*, *Phys. Rept.* **427** (2006) 257 [hep-ex/0509008] [INSPIRE].

[97] P. Janot and S. Jadach, *Improved Bhabha cross section at LEP and the number of light neutrino species*, *Phys. Lett. B* **803** (2020) 135319 [arXiv:1912.02067] [INSPIRE].

[98] A. Hook, E. Izaguirre and J.G. Wacker, *Model Independent Bounds on Kinetic Mixing*, *Adv. High Energy Phys.* **2011** (2011) 859762 [arXiv:1006.0973] [INSPIRE].

[99] D. Curtin, R. Essig, S. Gori and J. Shelton, *Illuminating Dark Photons with High-Energy Colliders*, *JHEP* **02** (2015) 157 [arXiv:1412.0018] [INSPIRE].

[100] C.M. Carloni Calame, M. Passera, L. Trentadue and G. Venanzoni, *A new approach to evaluate the leading hadronic corrections to the muon $g-2$*, *Phys. Lett. B* **746** (2015) 325 [arXiv:1504.02228] [INSPIRE].

[101] G. Abbiendi et al., *Measuring the leading hadronic contribution to the muon $g-2$ via μe scattering*, *Eur. Phys. J. C* **77** (2017) 139 [arXiv:1609.08987] [INSPIRE].

[102] G. Abbiendi, *Letter of Intent: the MUonE project*, CERN-SPSC-2019-026, SPSC-I-252 (2019).

[103] MUONE collaboration, *Status of the MUonE experiment*, *PoS* **ICHEP2020** (2021) 223 [arXiv:2012.07016] [INSPIRE].

[104] L. Di Luzio, A. Masiero, P. Paradisi and M. Passera, *New physics behind the new muon $g-2$ puzzle?*, *Phys. Lett. B* **829** (2022) 137037 [arXiv:2112.08312] [INSPIRE].

JHEP06(2022)122